Creation of a Site-Directed Mutant of Hen Egg White Lysozyme Working Toward Site-Specific Oxidation as it Relates to Protein Structure

by

Eric Mensah

Submitted in Partial Fulfillment of the Requirements

For the degree of

Masters of Science

in the

Chemistry

Program

Youngstown State University

August, 2009

Creation of a Site-directed Mutant of Hen Egg White Lysozyme Working Toward Site-Specific Oxidation as it relates to Protein Structure

Eric Mensah

I hereby release this thesis to the public. I understand that this thesis will be made available from OhioLINK ETD center and the Maag Library circulation Desk for public access. I also authorize the University or other individuals to make copies of this thesis as needed for scholarly research.

Signature:

Eric Mensah, Student Date

Approvals:

Dr. Michael A. Serra, Thesis Advisor Date

Dr. John A. Jackson, Committee Member Date

Dr. Peter Norris, Committee Member Date

Peter J. Kasvinsky, Dean of School of Graduate Studies & Research Date

Thesis Abstract

Metal catalyzed oxidation of protein involves a reaction between hydrogen peroxide and protein-bound metal ions. Production of the highly-reactive hydroxyl radical leads to oxidative damage in the immediate vicinity of the bound-metal ion. To examine the relationship between protein structure and oxidative damage a series of site-directed mutants of hen egg white lysozyme (HEWL) were created. This project focuses on generation of the site directed mutant where residue His15 will be altered to a serinyl residue (H15S), also work on the preliminary purification and characterization of the putative mutant would be touched on.

Acknowledgements

I would like to express my profound gratitude to my advisor, Dr. Michael Serra, for firstly accepting to be my advisor and whose keen interest, attention, care and driving force has made the timely completion of this work possible. I would also like to thank my committee members Dr. John Jackson and Dr. Peter Norris whose motivation can never be over emphasized. However, I am extremely grateful to Dr. Mincey for allowing me into his laboratory as much as I needed to use it.

I would also like to acknowledge and thank my family especially my wife, my mother, and my father for their emotional support and encouragements in all this period. I owe a lot to my brothers and sisters, for always calling to find out how life was treating me in a far away land, and also edging me on since education is the key to open life's mystery doors. I cannot end without showing my strongest appreciation to my best friend and mentor Christmas Wishart who was always there for me when I needed psychological help.

Finally, I realized that all these would have not come to pass without the financial support of the YSU School of Graduate Studies, and the esteemed faculty members of YSU Chemistry Department.

Table of Contents

List of Tables

Tables

List of Figures

Figures

List of Symbols and Abbreviations

ROS ..... Reactive Oxygen Species

H_2O_2 ..... Hydrogen peroxide

LOOH ..... Lipid peroxide

RNA ..... Ribose nucleic acid

DNA DNA ..... Deoxyribonucleic acid

Cu……Copper

Fe……Iron

M^{n+}…… Metal ion in the n^+ oxidation state

OH^-……Hydroxyl anion

M ..... Molar

s ..... Second

C……..Carbon

UV……Ultra violet

$^1\Delta GO_2$ ..... Singlet oxygen state

pKa ..... Ionization constant for a weak acid

pH……Hydrogen ion activity

GSH-Px ..... Glutathione peroxidase

NADPH ..... Nicotinamide adenine dinucleotide phosphate

MCO ..... Metal catalyzed oxidation

O_2……...Oxygen

His……Histidine

Ser……Serine

Zn……Zinc

SOD ..... Superoxide dismutase

OS ..... Oxidative stress

Ca……..Calcium

PKC……Protein kinase C

LDL .....Low density lipoprotein

DNPH 2,4-dinitrophenylhydrazine

cm……Centimeters

nm ..... Nanometer

V……Voltage

SDS ..... Sodium dodecyl sulfate

SDS-PAGE .....Sodium dodecyl sulfate-polyacrylamide gel electrophoresis

Tris……..Tris (hydroxymethyl) aminomethane

PCR.....Polymerase chain reaction

m ..... milli

ATP……..Adenosine triphosphate

µL……...Microliter

µg……..Microgram

S.O.C.....Super optimal broth

α ……alpha

AOX .....Alcohol oxidase

DHAS .....Dihydroxyacetone synthase

BSA.....Bovine serum albumin

OD .....Optical density

DMSO..... Dimethyl sulfoxide

PEG ..... Polyethylene glycol

YNB ..... Yeast nitrogen base

DI…….Deionzed water

rpm .....Revolution per minute

HPLC ..... High performance liquid chromatography

TAE……Tris-acetate-EDTA

AGC .....Serine

CAC ..... Histidine

kD……Kilo Dalton

HEWL ..... Hen egg white lysozyme

GAP.....Glyceraldehyde-3-phosphate

μM……...Micromolar

NEB.....New England Biolabs

CHAPTER I: INTRODUCTION

Reactive oxygen species (ROS) include the free radicals superoxide radical ($O_2^{\bullet-}$), and the hydroxyl radical ($HO^{\bullet}$), and non-radicals such as singlet oxygen, hydrogen peroxide (H_2O_2), and lipid peroxides (LOOH). The most reactive ROS by far is the hydroxyl radical which reacts under diffusion controlled rates causing oxidative damage to all types of biomolecules, including proteins, RNA, DNA, carbohydrates, and lipids. ROS have been implicated in many disease states such as premature aging, Alzheimer's disease, amyloid beta, amyotrophic lateral sclerosis, Parkinson's disease, Friedreich ataxia and Huntington's disease. Mutant proteins that block the transport of essential nuclear-encoded mitochondrial proteins to mitochondria, interact with mitochondrial proteins and disrupt the electron transport chain, induce free radicals, cause mitochondrial dysfunction, and ultimately damage neurons.[1, 2, 3]

ROS can be generated via various environmental and physiological pathways. Exogenous sources include ionization radiation or visible light in the presence of sensitizers, pollutants such as asbestos, ozone, and cigarette smoke. Endogenous sources include byproducts of aerobic respiration in the mitochondria, cytochrome, xenobiotics, and reactions involving transition metal ions and endogenously produced hydrogen peroxide. The reactions which involve transition metal ions such as Cu(I) and Fe(II) and hydrogen peroxide are the most important source of ROS *in vivo* (equation 1).[4]

$$M^{n+} + H_2O_2 \longrightarrow M^{(n+1)} + HO^{\bullet} + OH^{-} \qquad (1)$$

Oxidation is one of the major degradation pathways for protein pharmaceuticals. Methionine, cysteine, histidine, tryptophan, and tyrosine are the amino acid residues most susceptible to oxidation due to their high reactivity with various reactive oxygen species.

Oxidation during protein processing and storage can be induced by contaminating oxidants, which is catalyzed by the presence of transition metal ions and induced by light.[5]

Free Radicals and Reactive Oxygen Species

For many years the existence of free radicals in biological systems was dismissed as either non-existent or simply an unimportant curiosity. However, due to improved investigational techniques, this view has changed rather dramatically. A free radical is defined as a chemical species possessing an unpaired electron that can be considered as fragments of molecules and which are generally very reactive.[6] To attain stability a free radical abstracts a second electron from a neighboring molecule, leading to the formation of yet another free radical creating a self-propagating chain reaction.[7] Molecular oxygen is kinetically unreactive and it is readily reduced by an electron leading to the formation of partially reduced and reactive compounds collectively called reactive oxygen species. This is illustrated in equation 2.[8]

$$O_2 \xrightarrow{e^-} \underset{\text{Superoxide anion}}{O_2^{\bullet -}} \xrightarrow{e^- + 2H^+} \underset{\text{Hydrogen peroxide}}{H_2O_2} \xrightarrow{e^-} HO^- + \underset{\text{Hydroxyl radical}}{HO^{\bullet}} \xrightarrow{e^- + H^+} H_2O \qquad (2)$$

Several metal or metalloid ions exist in multiple oxidation states and can undergo electron transfer reactions that are important in biological and environmental systems. There are endogenous metal ions such as iron, copper and cobalt that participate in oxidation-reduction reactions with species including molecular oxygen, superoxide, and hydrogen peroxide. The well known Fenton reaction between endogenous iron and hydrogen peroxide generates the extremely reactive hydroxyl radical (equation 3).[5,9] Copper in the oxidation state of +1 undergoes a similar reaction with hydrogen peroxide.

$$Fe(II) + H_2O_2 \longrightarrow Fe(III) + OH^- + HO^{\bullet} \qquad (3)$$

A two step iron-catalyzed Haber-Weiss reaction emphasized how metal ions in the higher oxidation state are first reduced to catalyze the reduction of hydrogen peroxide to produce the corresponding hydroxyl radical (equation 4).

$$O_2^{\bullet-} + Fe(III) \longrightarrow Fe(II) + O_2$$
$$Fe(II) + H_2O_2 \longrightarrow Fe(III)\ OH^- + HO^{\bullet}$$
$$O_2^{\bullet-} + H_2O_2 \xrightarrow[\text{Fe catalyst}]{} O_2 + OH^- + HO^{\bullet} \qquad (4)$$

Reactive oxygen species are unavoidable intermediates of metabolic processes of living organisms and they may not always be harmful. Their positive actions include, involvement in killing bacteria by phagocytic cells and participation in platelet aggregation.[10] There are, however, suggestions that the imbalance between their synthesis and neutralization may initiate lipid peroxidation which is the basis of the etiology of many different illnesses.[11] The most reactive of them all is the hydroxyl radical. $HO^{\bullet}$ reacts at diffusion controlled rates, causing oxidative damage to all classes of biological molecules. Almost every molecule in the cell will react with the electrophilic $HO^{\bullet}$ with second order rate constants of 10^9 - 10^{10} M^{-1} sec^1. Ions of iron, copper, cobalt, and manganese are the most physiologically studied transition elements involved in the production of ROS. The kinetic data of rate constants indicate that proteins are major targets of $HO^{\bullet}$. For instance, the rate constant of collagen with $HO^{\bullet}$ is on the order of 4 x 10^{11} $M^{-1}s^{-1}$, DNA 8 x 10^8 $M^{-1}s^{-1}$ and albumin 8 x 10^{10} $M^{-1}s^{-1}$. Proteins are the main target of oxidative damage by ROS due to the fact that they are the components of biological molecules.[11,12]

Radiation in the form of ultraviolet light (UV), gamma rays, microwaves, and X-rays through homolytic fission of water molecules generates the hydroxyl radical. UV can produce singlet oxygen. Singlet oxygen is formed when pigments are exposed to radiation in the presence

of oxygen. This happens when oxygen, in its lowest energy state, absorbs energy to form the excited singlet oxygen states ($^1\Delta GO_2$). Singlet oxygen states can also be produced in biological systems by reaction between H_2O_2 and hypochlorite resulting from phagocyte acidity, the interaction between light and chlorophyll, and as a consequence of the interaction between light and rhodopsin in the eye. For example, patients with porphyrias are sensitive to light and produce excessive ($^1\Delta GO_2$).[4] In the laboratory $^1\Delta GO_2$ can be formed either chemically by reaction between H_2O_2 and hypochlorite or photochemically through the reaction between O_2 and dyes such as acridine orange or methylene blue.

The addition of one electron to oxygen yields the superoxide free radical anion, $O_2^{\bullet-}$. The superoxide radical anion can be produced by exposing oxygen to ionization radiation or as part of normal metabolism. For example, catabolism of xanthine to uric acid catalyzed by xanthine oxidase as well as other flavoproteins. It is deliberately produced during the respiratory burst of phagocytic cells, forming part of the body's defense system for the destruction of invading organisms. Traces of $O_2^{\bullet-}$ are formed when O_2 combines with hemoglobin and myoglobin and a considerable quantity of $O_2^{\bullet-}$ is accidentally formed in the mitochondria when oxygen is reduced to water.

$O_2^{\bullet-}$ is a base and thus accepts protons, forming the more reactive hydroperoxyl radical ($HO_2^{\bullet}$). The pKa of this reaction is ~4.5 such that under physiological conditions only one $HO_2^{\bullet}$ molecule exists for every 100 $O_2^{\bullet-}$ molecules. $HO_2^{\bullet}$ synthesis from $O_2^{\bullet-}$ is pH sensitive and is favored by acidic conditions. Although at physiological pH the abundance of $HO_2^{\bullet}$ is rather low its level will increase when the pH decreases, for instance, following ischemia or severe acidosis or in close proximity to the cytosolic side of the inner mitochondrial membrane. $HO_2^{\bullet}$ is more reactive than $O_2^{\bullet-}$ and due to its lipophilicity, would be expected to be able to cross biological

membranes as effectively as H_2O_2.[5] This is important, because, unlike $O_2^{\bullet-}$, it can initiate peroxidation of polyunsaturated fatty acids directly. However, $HO_2^{\bullet}$ is still a very poor initiator and there is little evidence that it can cause such damage *in vivo.* The level of $O_2^{\bullet-}$ is mainly controlled by both spontaneous and enzymatic dismutation producing hydrogen peroxide (equation 5).

$$2O_2^{\bullet-} + 2H^+ \longrightarrow H_2O_2 + O_2 \qquad (5)$$

Hydrogen peroxide is a non-radical ROS found in biological systems that is produced by several different enzymatic reactions, including those catalyzed by d-amino acid oxidase, amine oxidase, glycollate oxidase, ureate oxidase and superoxide dismutase. H_2O_2 is also formed during redox cycling of compounds such as the catecholamines, from microsomal cytochrome P-450 during the processing of fatty acids and xenobiotics, from the respiratory burst of phagocytes, and from mitochondrial respiration. H_2O_2, like $O_2^{\bullet-}$, is only a weak oxidizing agent and not very reactive *in vivo*. It will react with thiols and by so doing can inactivate enzymes that contain an essential thiol group, such as the glycolytic enzyme glyceraldehydes-3-phosphate dehydrogenase. Unlike $O_2^{\bullet-}$, H_2O_2 can readily cross cell membranes and if it encounters Fe^{2+} or Cu^+ will form the more aggressive $HO^{\bullet}$.[4, 14]

Several assays have been developed to detect and estimate $HO^{\bullet}$ in biological systems. These assays detect the products of $HO^{\bullet}$ oxidation such as the production of ethane from methional (3-methylthiopropionaldehyde) and related compounds, formation of degradation products from tryptophan, production of methanesulfanic acid from dimethylsulfoxide, production of radio-labeled CO_2 from [carboxy-^{14}C]benzoic acid, and deoxyribose assay, a simple "test-tube" assay for determination of rate constants for reactions of hydroxyl radicals.

Anti-oxidant Defense Mechanisms

A number of antioxidants have evolved to scavenge ROS. An antioxidant is any substance that when present at low concentrations compared with that of an oxidizable substrate significantly delays or inhibits oxidation of that substrate. Glutathione peroxidase (GSH-Px) is found in human tissues such as lungs, liver, platelets, and erythrocytes.[10] This enzyme requires the presence of Se and free thiol groups for catalytic activity. It controls the speed of lipid peroxidation, protects cell membranes against peroxidative damage, ensures correct cell metabolism by taking part in the regulation of many processes such as the pentose cycle. Its main role is the removal of H_2O_2 by converting it to water. As a result, oxidized glutathione is formed. The oxidized glutathione is reduced by NADPH requiring glutathione reductase. Superoxide dismutase (SOD) was first isolated in 1939 from bovine erythrocytes. It was the first enzyme discovered whose substrate was a free radical.[2] Its main role is to remove $O_2^{\bullet-}$ by accelerating its conversion to H_2O_2. Catalases in the liver, kidney, and erythrocytes dispose of H_2O_2 by converting it to water and O_2. Another important enzyme that sequesters transition metal ions such as Fe(II) is transferrin which plays an essential role in iron metabolism. A glycoprotein produced in the liver, transferrin binds Fe(III) tightly but reversible. At low pH transferrin releases the Fe(III) in the cell's vesicles thereby preventing an iron overload of the cell.[16] Sometimes these protective mechanisms are disrupted by various pathological processes, and antioxidant supplements such as vitamins A, D, and E are vital to combat oxidative damage. Although the availability of catalytically active forms of iron and copper are very low *in vivo,* when free metal ions do become available they do not exist in the free state for long, they either bind to other molecules or precipitate out of solution as hydroxide or phosphate salt.[17] Most amino acids are susceptible to oxidative damage due to their low oxidative potential. Methionine

is readily oxidized to methionine sulfide by ROS with a second order rate constant of 8.5 x 10^9 $M^{-1}s^{-1}$. The repair enzyme methionine sulfoxide reductase is capable of reducing the oxidized form back to the reduced form. This redox reaction is believed to play a role in protecting other functional residues from oxidative damage thus functioning as an antioxidant. The antioxidant function of methionine in proteins is not limited only to proteins but functions in the reduction of cholesterol esters and hydroperoxides to alcohols by high density lipoproteins. [12, 18]

Metal Catalyzed Oxidation and Site-specific Oxidation

The reaction between metal ions and hydrogen peroxide or O_2 to form the hydroxyl radical is referred to as metal-catalyzed oxidation (MCO). Depending upon the electron donor system used, the reduction of O_2 can proceed by a two-electron mechanism yielding H_2O_2 directly, or by way of two sequential one-electron transfer processes leading to the formation of the superoxide anion followed by its dismutation to H_2O_2 and O_2. Similarly, the reduction of Fe(III) to form Fe(II) can occur directly or via the intermediate formation of the superoxide anion, which can react directly with Fe(III) given Fe(II) and O_2. It is believed that the Fe(II) then binds to a metal-binding site on the protein after which the protein-iron complex reacts with the H_2O_2 to generate *in situ* a reactive oxygen species, which reacts with side chains of amino acid residues in the immediate vicinity of the metal-binding site. The MCO-catalyzed oxidation reaction of proteins is a site-specific process involving the interaction of H_2O_2 and Fe(II) or Cu(I) at the metal binding sites of the protein. The site-specific nature of the reaction is indicated by the following facts: (*a*) the inactivation of enzymes by MCO systems is relatively insensitive to inhibition by free radical scavengers, (*b*) only one or at most only a few amino acid residues in the protein can be modified when proteins are subjected to free radicals, (*c*) most of the enzymes that are highly sensitive to modification by MCO systems require metal ions for

activity, therefore, they must contain a metal binding-site, and (*d*) in the case of *E. coli* glutamine synthetase, the loss of catalytic activity correlates with loss of a single histidyl and a single arginyl residue per unit, both of which are situated in close proximity to one of two divalent metal binding sites on the enzyme.[20] Studies have also shown two histidyl residues, His18 and His21, which are sensitive to oxidation in human growth hormone, are located in close proximity to a metal ion binding site. Surface exposed histidyl residues which do not form part of a metal-binding site resist MCO systems. Site-specific oxidation has also been observed in enzyme systems such as Cu, Zn superoxide dismutase (Cu, Zn SOD), and *in vitro*, Fe(II) dehydrogenases, glycated insulin, and low density lipoprotein (LDL). In fact, conversion of histidine especially to 2-oxo-His has been suggested as an important marker for oxidative stress *in vivo*.[21]

Oxidative Stress

Oxidative stress is caused by the presence of reactive oxygen species which the cell is unable to counterbalance. The result is damage to one or more biomolecules including DNA, RNA, proteins and lipids. Generally, ROS generation and antioxidant defense mechanisms are in a balance and in cases such ischemia/reperfusion the balance favors ROS production resulting in oxidative damage to biomolecules. Such damage includes protein carbonyl formation, modification of amino acid residues, covalent cross-linking, and fragmentation of the polypeptide chain. Oxidative stress (OS) induces cellular injury by the production of free radicals of high reactivity, leading to membrane lipid peroxidation and oxidation of critical thiol groups, causing formation of homo- and hetero-proteins bound by disulfide bridges and inhibition of their function.[22, 23] De Monte, *et al.* accumulated evidence indicating that OS is involved in hepatopathies such as ischemic liver, alcoholism, steatohepatitis and pathologies leading to

hepatic iron accumulation among others.[23] It is also believed that OS elevates Ca^{2+} and presumably activates Ca^{2+} dependant protein kinase C (PKC), an effect causing cellular injury.[22] Elevated levels of protein carbonyls are found in many disease states such as rheumatoid arthritis and in cataractogenesis.[19] MCO products of low density lipoproteins (LDL) have been implicated in atherosclerosis, a condition of chronic inflammatory response in the walls of arteries, in large part due to the accumulation of microphage white blood cells and promoted by LDLs. The presence of iron in atherosclerotic plaques has been found and is believed to be an important modulator of lipid peroxidation. Accumulation of protein carbonyls have been implicated in aging.[19] Relationships have been found between the content of protein carbonyls and the cell in human erythrocyte and in cultured fibroblast,[25] and between the content of protein carbonyls and subject age in human brain and in the lens tissue of the eye. Also, in various diseases, the rise in protein carbonyls has been demonstrated such as premature aging, muscular dystrophy, respiratory distress syndrome, amyotrophic lateral sclerosis and diabetes. Furthermore, histological distribution of protein carbonyls in diseases has been determined in the brain tissues of patient with Alzheimer's disease.[26]

Since oxidative stress leads to an increase in the levels of protein carbonyls, the formation of protein carbonyls is used as a measure of oxidative damage in various physiopathological conditions. Several assays have been developed to measure protein carbonyls. At present protein carbonyls are generally measured spectrophotometrically using 2,4-dinitrophenylhydrazine (DNPH), which has an absorbance maximum at 370 nm and a molar extinction coefficient of 22,000 $M^{-1}cm^{-1}$. Over the past 20 years the effect of aging and various pathological processes on the levels of carbonyl protein extracts from tissues of laboratory rodents and human subjects have been studied.[27] More recently, methods using western blots

have been developed to identify specific proteins showing increased levels of carbonyls. Chaudhuri *et al.* have been able to quantify the protein carbonyls on specific proteins in the cytosol of liver using a fluorescence-based assay which employs 2-D gel electrophoresis and mass spectrometry.[27]

Giulivi *et al.* proposed dityrosine as a biomarker for oxidative stress.[29] Dityrosine (tyrosine-tyrosine bonding) is found in several proteins as a result of UV irradiation, γ-irradiation, aging, and exposure to oxygen free radicals.[28] Although carbonyl assays can be used as a measure of protein oxidation, it must be noted these moieties may also be introduced into proteins by mechanisms that do not involve the oxidation of amino acid residues. For example, α,β-unsaturated alkenals produced during lipid peroxidation may react with sulfhydryl groups of proteins to form stable covalent thioether adducts carrying carbonyl groups. It is noteworthy that aromatic amino acids in proteins are not major sites of oxidation by MCO systems, whereas phenylalanine, tryptophan, and tyrosine are preferred targets by radicals produced during γ-radiolysis. These differences in specificity result from the chemical structure of the amino acids with putative binding sites for metals. In the presence of oxygen, considerable peptide cleavage occurs, with concomitant formation of carbonyl groups. Under hypoxic or anoxic conditions, hydroxyl radicals produced during radiolysis leads to extensive protein-protein cross-linkage via dityrosine and possibly other amino acid cross-linking (e.g., disulfide bridge). Thus, specific post-translational modifications of amino acids in proteins are necessary to assess cellular or organismal injury under different oxidative stress conditions. It is believed that covalent modification of amino acids may serve as a "marking" step for protein degradation. The only protein modification obtained under various conditions of oxidative stress and consistent with simple laboratory techniques is the formation of dityrosine.[28] Dityrosine is an unusual amino acid

that is distinguished by the intense 420 nm fluorescence, measurable upon excitation within either 312 nm (alkaline solutions) or 284 nm (acidic solutions) absorption bands. Dityrosine formation begins with the generation of a tyrosyl radical, radical isomerization followed diradical reaction, and finally enolization with overall rate constant for the process reported as 4×10^8 M^{-1} s^{-1}.[29] Thus the initial step in the formation of dityrosine involves the formation of a tyrosyl radical. The reduction potential of the tyrosine$O^{\bullet}$/tyrosineOH couple is 0.88V[30] indicating that the coupled reaction needs to be highly oxidative to be thermodynamically favorable. Species such as hydroxyl radical are required to fulfill this condition. Once the tyrosyl radical is formed, the production of dityrosine involves two monomeric molecules of tyrosine-containing proteins, joined by intermolecular cross-linking. The resulting protein dimer is detectable by SDS-PAGE under suitable conditions. Dityrosine has also been proposed as a marker of organismal oxidative stress. Dityrosine concentrations were found to be 100-fold higher in LDL isolated from atherosclerotic lesions than normal ones.[31] Also, humans suffering from systemic bacterial infections had twice the concentration of dityrosine in urine than those of healthy individuals.[31]

Methionine sulfoxide, an oxidative product of methionine is another potential marker for oxidative stress, and it has been detected in many disease states *in vivo*.[12]

Protein Modification

Several lines of evidence indicate that oxidative modification of protein and the subsequent accumulation of oxidized proteins, which could be an early indication of oxygen radical-mediated tissue damage, have been found in cells during aging, oxidative stress, and in various pathological states including premature diseases, muscular dystrophy, rheumatoid arthritis, and atherosclerosis. Various protein modifications including cross-linking, peptide bond cleavage, oxidation of amino acid side chain, and protein carbonylation have been extensively studied.

Cross-linking

Oxidative modification of proteins can give rise to intra- or inter-protein cross-linked derivatives by several different mechanisms such as the formation of dityrosine. Extensive dityrosine can be found in several proteins when exposed to UV radiation in the presence of oxygen radical (Figure 1-1).

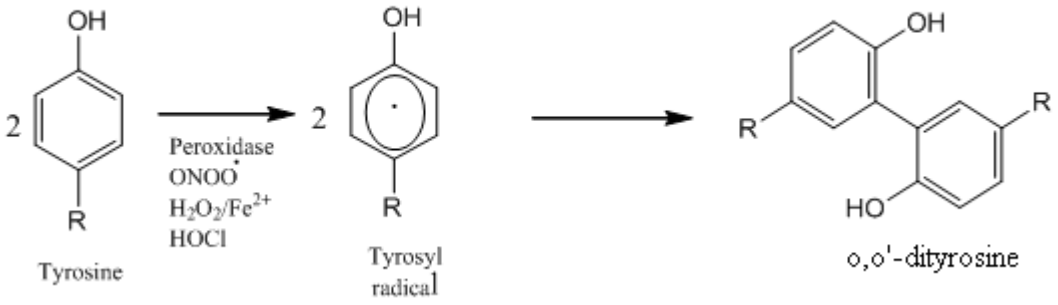

Figure 1-1: Proposed reaction mechanism of dityrosine formation

In the literature one can find at least five other pathways that can result in the formation of inter-protein cross-linkages.[1]

1. Carbon-carbon covalent linkages are formed by the direct interaction of two carbon-centered radicals of protein derivatives formed on oxidation of the protein backbone or the amino acid side-chains (equation 6).

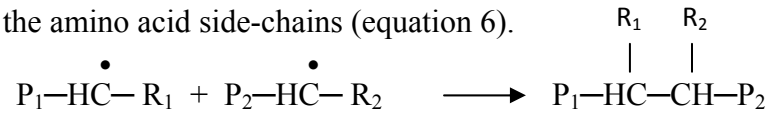

$$P_1{-}\overset{\bullet}{H}C{-}R_1 + P_2{-}\overset{\bullet}{H}C{-}R_2 \longrightarrow P_1{-}HC(R_1){-}CH(R_2){-}P_2 \quad (6)$$

2. Interaction between malondialdehyde and other dialdehydes with amino groups of lysine residues in two different protein molecules (equation 7).

$$P_1\text{-}NH_2 + P_2\text{-}NH_2 + CH_2(CHO)_2 \longrightarrow P_1\text{-}N{=}CHCH_2CH{=}N\text{-}P_2 + H_2O \quad (7)$$

3. Interaction of the products of Michael addition (product of interaction between 4-hydroxy-2-nonenal, HNE) with any protein of an amino group lysine residue and lysyl residue of a second protein molecule (equation 8).

$$P^1\text{-HNE-CHO} + P^2\text{-}NH_2 \longrightarrow P^1\text{-HNE-CH}{=}N\text{-}P^2 + H_2O \quad (8)$$

4. Interaction of carbonyl group of products of glycation of one protein with lysyl residue amino of a second protein (equation 9).

$$P^1R_1CHO + P^2\text{-}NH_2 \longrightarrow P^1R_1\text{-CH}{=}N\text{-}P^2 + H_2O \quad (9)$$

5. Oxidation by cysteine residue reactive species (RS) of two different proteins (equation 10).

$$P^1SH + P^2SH + RS \longrightarrow P^1S\text{-}SP^2 + \text{reduced RS} \quad (10)$$

Peptide Bond Cleavage

The oxidation of proteins by ROS can lead to the cleavage of peptide bonds.[32] The alkyl radicals, alkoxyl radicals and alkylperoxide intermediates of protein oxidation by hydroxyl radical can undergo cleavage by either α-amidation or diamide pathways (Fig.1-2).

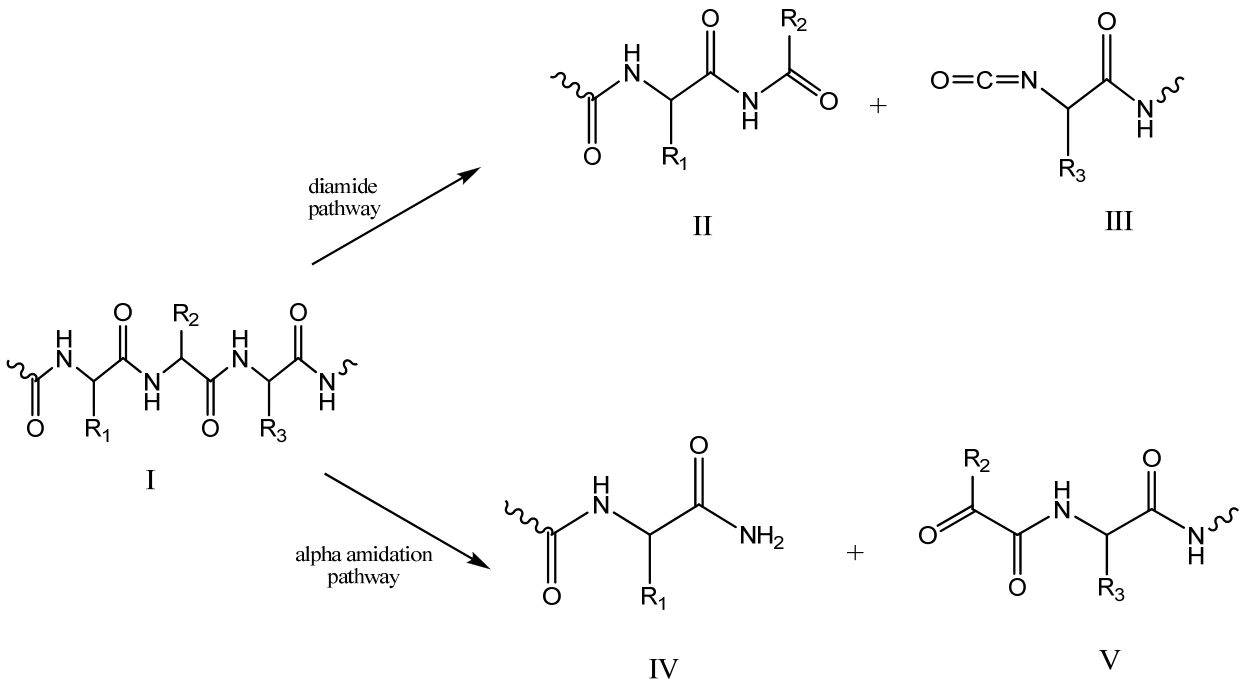

Figure 1-2: Cleavage of the polypeptide chain by the diamide or the α-amidation pathway.

In the α-amidation pathway, the C-terminal amino acid of the fragment derived from the N-terminal region of the protein will exist as an amide derivative (IV) and the N-terminal amino acid of the fragment derived from the C-terminal portion of the protein will exist as an α-keto-acyl derivative (V). In contrast, the C-terminal amino acid of the fragment derived from the N-terminal portion of the protein via the diamide pathway will exist as the diamide derivative (II) and the N-terminal amino acid residue of the peptide fragment derived from the C-terminal region of the protein will exist as the isocyanate derivative (III).[18]

The oxidation of glutamyl and aspartyl residues of proteins can also lead to peptide bond cleavage in which the N-terminal amino acid of the C-terminal fragment will exist as the N-pyruvyl derivative (Figure1-3).[18]

A.

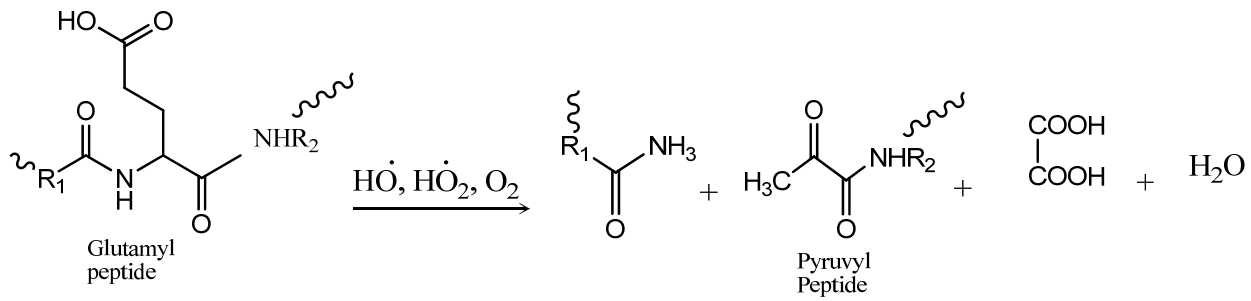

B.

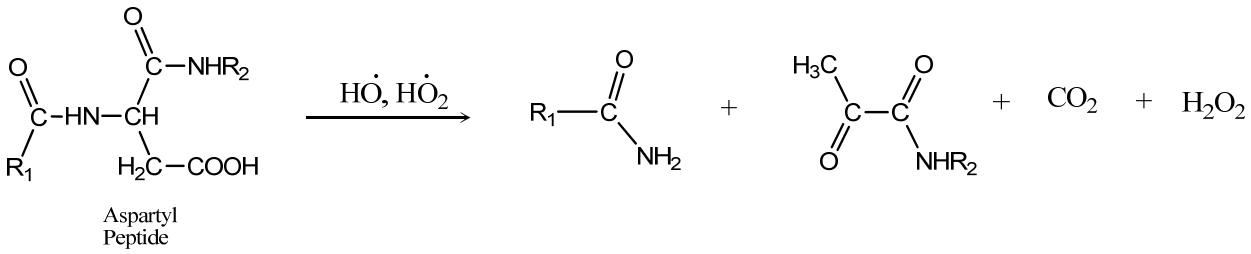

Figure 1-3: Oxidative cleavage of a glutamyl residue (A) and an aspartyl residue (B).

In addition, based on findings that the number of peptide fragments formed in the radiolysis of proteins is approximately equal to the number of prolyl residues, Schuessler and Schilling (1984),[33] proposed that oxidation of prolyl residues leads to peptide bond cleavage. This was subsequently confirmed by Uchida, *et al.* (1990),[34] showing that oxidation of proline residues can lead to peptide bond cleavage by a mechanism that involves oxidation of the proline residue to a 2-pyrrolidone derivative (Figure 1-4 A). It is noteworthy that acid hydrolysis of 2-pyrrolidone yields 4-aminobutyric acid (Figure 1-4 B). Thus, the presence of 4-aminobutyric acid in protein hydrolysates might be a measure of cleavage by the prolyl oxidation pathway.

A.

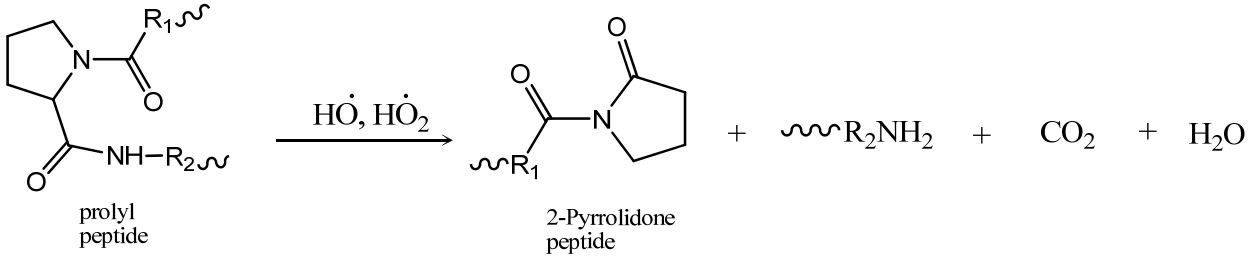

B.

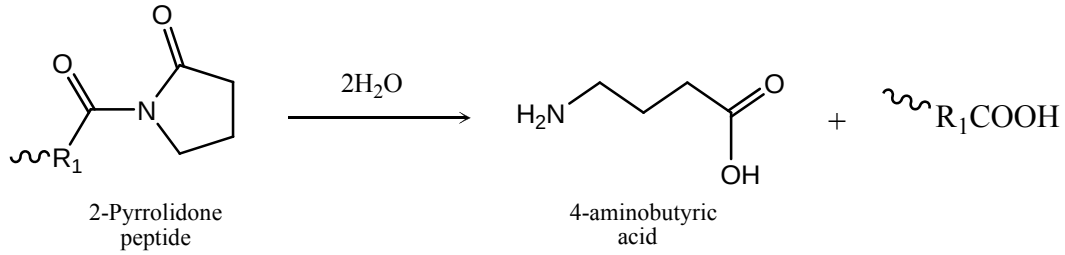

Figure 1-4: Polypeptide bond cleavage by oxidation of prolyl residues (A) and acid hydrolysis of 2-Pyrrolidone (B).

Oxidation of amino acid residue side chains

All amino acid residues of peptides are susceptible to oxidation by the hydroxyl radical; [1] however, the products are characterized in only a few cases. To simplify the analysis of the modified product formed, the side chain amino acids have been grouped as: aromatic amino acids, sulfur containing groups and amino acids which oxidize to give carbonyl groups. Aromatic amino acid residues are particularly susceptible to oxidation by ROS. Under these conditions phenylalanine is converted to both mono- and dihydroxy derivatives and tyrosine is converted to the 3,4-dihydroxy derivative. Tryptophan is highly sensitive to oxidation by γ-radiation, which leads to various hydroxy derivatives, formyl-kynurenine, and 3-hydroxy-kynurenine. It is

believed that tyrosine and tryptophan residues are not major targets in systems with physiological concentrations of transition metal ions. Supposedly these residues are usually not present at metal-binding sites of proteins. In contrast to tyrosyl and tryptophanyl residues, histidinyl, argininyl, and lysyl residues are highly sensitive targets for free radical induced oxidation in systems with physiological concentration of transition metal ions. It is assumed that this is due to their localization in the metal-binding sites of proteins. Oxidation of histidine generates the 2-oxo-histidine and its ring-ruptured products (4-hydroxy glutamate, aspartate, and asparagine), whereas oxidation of lysine generates carbonyl products including aminoadipic semialdehyde.[1,47] Proline residues are oxidized to glutamic semialdehyde, pyroglutamic acid, 2-pyrrolidone, and 4- and 5-hydroxy derivatives. Though cysteine and methionine residues in proteins are particularly susceptible to oxidation by all forms of ROS systems, in contrast to other amino acid residues, the partially oxidized forms of cysteine and methionine can be reduced by specialized enzymatic systems. Cysteine residues of certain peroxiredoxins undergo reversible oxidation to sulfinic acid (Cys-SO_2H) and the reduction reaction is catalyzed by sulfiredoxins.[38]

Protein carbonylation

As illustrated in Figures 1-3 and 1-4, direct reaction of proteins with ROS can lead to formation of protein derivatives or peptide fragments possessing highly reactive carbonyl groups (ketones, aldehydes). As indicated in Figure 1-5, proteins containing reactive carbonyl groups can also be generated by secondary reactions of primary amino groups of lysine residues of proteins with reducing sugars or their oxidation products (glycation/glycoxidation reactions),[18] and also by Michael-addition reactions of lysyl, cysteinyl, or histidinyl residues with α,β-unsaturated aldehydes formed during the peroxidation of polyunsaturated fatty acids. Since the

presence of protein carbonyl derivatives in cells reflects damage induced by multiple forms of ROS, a number of analytical procedures have been developed to determine the protein carbonyl content of biological materials.

A.

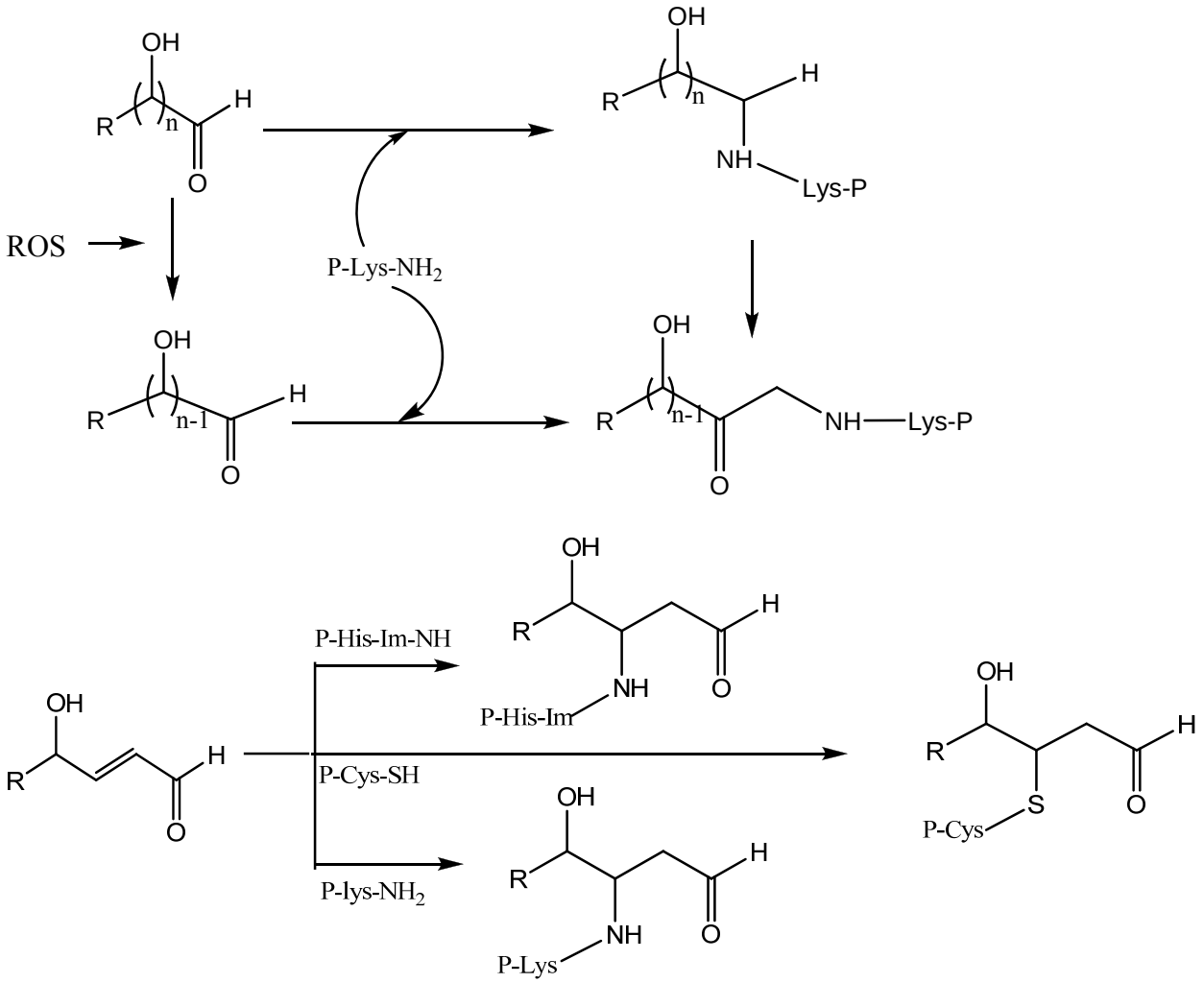

Figure 1-5: Generation of carbonyl derivatives of proteins: (A) by glycation/glycoxidation of lysine amino groups and (B) by reactions of α,β-unsaturated aldehydes with lysine, cysteine, and histidine residues of proteins.

Conformational Changes and Effects on Structure and Function of Proteins

Oxidation of the side chain of amino acids can lead to unfolding and conformational changes in proteins which consequently affect their functions. Studies have shown that oxidation of more surface exposed residues have less effect on protein structure and conformation, than does oxidation of more buried amino acid residues. Solvent-accessible methionine residues are much more readily oxidized than the buried residues in bovine growth hormone.[35] Oxidation of surface exposed methionine residues do not affect the conformation of most proteins unless the residues are found in a pocket. In effect oxidation of buried methionine residues affect the protein structure. The role of methionine oxidation in the loss of catalytic activity was studied by site-directed mutagenesis of subtilisin, a mutant protein with Met222 changed to Ser, Ala, or Leu which is resistant to oxidation by high concentration of hydrogen peroxide.[12] This was to minimize the increasing inactivity of the protein due to the susceptibility of Met222 to oxidation.

Oxidation of histidine leads to the formation of 2-oxo-histidine which is further oxidizes to generate the ring-opened products, such as aspartate, aspartylurea and formylasparagine. Therefore, histidine oxidation in effect, may change protein conformation since its oxidation results in loss of basicity of the side chain residue, and thus alters the net charge on the protein and consequently affect the isoelectric point of the protein and its hydrophobicity.

Statement of the Research Problem

Reactive oxygen species including the superoxide radical, hydroxyl radical, singlet oxygen and hydrogen peroxide, are well known cytotoxins have been implicated in the etiology of a wide range of diseases that affect human beings. The highly reactive hydroxyl radical is formed when transition metal ions including Fe^{2+} and Cu in the +1 state react with hydrogen

peroxide. The reaction between hydrogen peroxide and the transition metal ions is referred to as metal- catalyzed oxidation. Some researchers argue that site-specific damage caused by metal catalyzed oxidation system results from a "caged" reaction in which the metal ion binds in pockets found along the surface of the protein. The pocket provides a protective environment for the production of ROS preventing them from being scavenged by the antioxidant defense system *in vivo*. It is also known that copper binds histidine residues tightly, and; therefore, oxidative damage occurs frequently around histidyl residues in a protein, and it might be expected that oxidative damage would occur more often around histidyl residues in protein.[35]

This argues that the primary structure may be most important in determining a proteins susceptibility to metal-catalyzed oxidation. This research examines whether a proteins primary sequence or tertiary structure is most important in site-specific oxidation. The purpose of this thesis was to generate a site-directed mutant of hen egg white lysozyme where residue His15 (Figure: 1-6) was altered to a serinyl residue (H15S). The thesis will also present work on the expression, preliminary purification, and its characterization of the mutant protein.

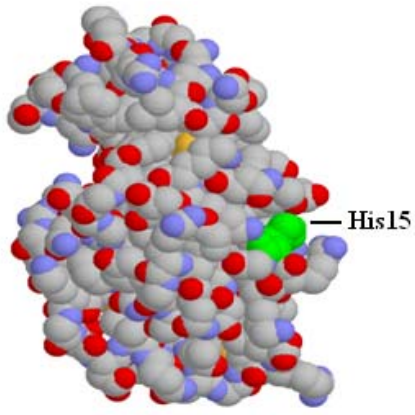

Figure 1-6: Structure of hen egg white lysozyme highlighting the position of the only histidyl residue.

CHAPTER II: MATERIALS AND METHODS

Section I: Generation of the Mutant Gene by Site-directed Mutagenesis

A single site-mutant was generated by the PCR overlap extension method. This gene was generated and cloned into pCR®4-TOPO® (Invitrogen) previously by Anitha Muttavarapu. The mutant with histidine at position 15 was changed to serine. An alteration of the 5' end allowed for incorporation of the gene in frame with the α-factor signal sequence found on the vector pPICZα A. The gene was sub-cloned into the pPICZα A, and used to transform TOP10 *E. coli.*

pPICZα A Cloning Reaction and Chemical Transformation

The mutant gene was cloned into the yeast vector pPICZα A (Figure 2-1). The reaction mixture included 20 ng of the mutant gene (H15S) obtained from the PCR of the H15S-pCR®4-TOPO® construct, 40 ng (4 µL) of pPICZα A (Invitrogen), 4 µL 5x Buffer (250 mM Tris-HCl, pH 7.6, 50 mM $MgCl_2$, 5 mM ATP, 5 mM dithiothreitol, 25% (w/v) polyethyleneglycol-8000), 1 µL 10 mM ATP, 1µL T4 DNA ligase (New England Biolabs), and nuclease free water (Promega) for a total volume of 20 µL. The reaction mixture was incubated at room temperature for 2 hours. 2 µL of the pPICZα A cloning reaction was added to 50 µL of One Shot® chemically competent *E. coli* cells in a 2 mL microcentrifuge tube. The mixture was gently mixed and then incubated on ice for 30 minutes. The cells were immediately heat shocked at 42 °C without shaking for 30 seconds and the tubes were carefully transferred back to ice. 250 µL of S.O.C (super optimal broth) medium at room temperature was added to each tube, capped tightly, and shaken horizontally at 200 rpm and 37 °C for 1 hour. 30 µL of the cells plus 20 µl of S.O.C medium was spread on prewarmed low salt LB plates containing 25 µg/mL of Zeocin™ and incubated overnight at 37 °C. Ten colonies (EcoxA1, EcoxB2, EcoxC3, EcoxD4, EcoxE5,

EcoxF6, EcoxG7, EcoxH8, EcoxI9, and EcoxJ10) were selected and individually streaked on fresh low salt LB plates with Zeocin™ for analysis of insert. Each colony was inoculated into 2 mL low salt LB broth with Zeocin™ and grown overnight at 37 °C with vigorous shaking at 250 rpm. The plasmid was isolated from the overnight culture using a QIAprep® Miniprep Kit (50).

Analysis of plasmids for insert by PCR

50 ng of freshly isolated plasmid was thoroughly mixed with 10 µL of GoTaq™ Green Master Mix (Promega), 1 µL each of the primers 10 µM 5' AOX1 and 10 µM 3' AOX1 (Figure 2-1), and then sterile water to bring the final volume to 20 µL. The PCR cycling program included an initial denaturation temperature of 95 °C for 2 minutes. This is followed by denaturation at 95 °C for 1 minute, annealing at 50 °C for 30 seconds, and extension for 1 minute at 72 °C for 30 cycles. The final extension was held at 72 °C for 10 minutes. The PCR products were analyzed on a 1% agarose gel at 85 V for 70 minutes. The gel was soaked in ethidium bromide to visualize the DNA. Samples containing the plasmid were then sequenced.

A. 5'-GACTGGTTCCAATTGACAAGC-3'

B. 5'-GCAAATGGCATTCTGACATCC-3'

Figure 2-1: 5' *AOX1* sequencing primer (A) and 3' AOX1 sequencing primer (B)

Analysis of plasmids for insert by restriction digests

To further analyze for positive transformants, 100 ng of isolated plasmid was digested with 2 µL of 1 mg/mL BSA, 2 µL NEB buffer # 2, 2 µL *XhoI* and sterile water to obtain a final volume of 20 µL. The reaction mixture was incubated at 37 °C for 2 hours, and then characterized by 1% agarose gel. Uncut plasmid was run as the control.

Sequencing

Plasmids from colonies EcoxA1, EcoxC3, EcoxE5, EcoxF6, EcoxH8, and EcoxJ10 were prepared for sequencing according to the Beckman Coulter CEQ 2000 Dye Terminator Cycle sequencing kit, and sequencing was performed on a Beckman Coulter CEQ 2000 XL DNA analysis system. The reaction mixture contained 7 μL (70 ng) of DNA templates, 2 μL sequencing primer (1.6 μM 5' AOX1), 8 μL DTCS Quick Master Mix, and 3 μL deionized water. The thermal cycling program consisted of three steps as follows: 96 °C for 20 seconds, C.50 °C for 20 seconds, 60 °C for 4 minutes, repeated 30 times and finally held at 4 °C. The reaction was quenched with 4 μL stop solution (1.5 M NaOAc + 50 mM EDTA) with 1 μL of 20 mg/ml of glycerol and the DNA precipitated with cold 95% ethanol. The pellet was then rinsed with cold 70% ethanol, vacuum dried, and dissolved in 40 μL sample loading buffer before loading into the CEQ.

Section II: Transformation and Expression of Protein in *Pichia pastoris*

Pichia pastoris is quite similar to *Saccharomyces cerevisiae* as far as general growth conditions and handling. *Pichia pastoris* is an industrial methylotrophic yeast that was initially chosen for production of single cell proteins because of its ability to grow to very high cell density in simple defined media. This fermentation technology formed the basis of a highly efficient expression system using the methanol-inducible *AOX1* promoter and vectors that integrate into the *P. pastoris* genome.[36] The increasing popularity of this expression system can be attributed to several factors, most importantly: (1) the simplicity of techniques needed for the molecular genetic manipulation of *P. pastoris* and their similarity to those of *Saccharomyces cerevisiae,* one of the most well-characterized experimental systems in modern biology; (2) the

ability of *P. pastoris* to produce foreign protein at high levels, either intracellularly or extracellularly; (3) the capability of performing many eukaryotic post-translational modifications, such glycosylation, disulfide bond formation and proteolytic processing; and (4) the fact that the expression system is a commercially available kit.

P. pastoris metabolizes methanol as a source of carbon and energy. Biochemical studies have shown that methanol utilization requires a novel metabolic pathway involving several unique enzymes. The enzyme alcohol oxidase (AOX) catalyses the first step in the methanol utilization pathway, the oxidation of methanol to formaldehyde and hydrogen peroxide. AOX is sequestered within the peroxisome along with catalase, which degrades H_2O_2 to oxygen and water. A portion of the formaldehyde generated by AOX leaves the peroxisome and is further oxidized to formate and carbon dioxide by two cytoplasmic dehydrogenases, reactions that are a source of energy for cells growing in methanol. The remaining formaldehyde is assimilated to form cellular constituents by a cyclic pathway that starts with the condensation of formaldehyde with xylulose 5-monophosphate, a reaction catalyzed by a third peroxisomal enzyme dihydroxyacetone synthase (DHAS). The products of this reaction, glyceraldehyde 3-phosphate and dihydroxyacetone, leave the peroxisome and enter the cytoplasmic pathway that regenerates xylulose 5-monophosphate, and for every three cycles, one net molecule of glyceraldehyde 3-phosphate is produced. Two of the methanol pathway enzymes, DHAS and AOX, are present at high levels in cells grown on methanol but are not detectable in cells grown on most other carbon sources (glucose, glycerol, or ethanol). In cells fed with methanol in fermenter cultures, to ascertain growth-limiting rates, AOX levels were dramatically induced, constituting >30% of total soluble proteins.[36, 37]

There are two genes that encode alcohol oxidase activity in *P. pastoris*: *AOX1* and *AOX2*; *AOX1* is responsible for the vast majority of alcohol oxidase activity in the cell. Expression of the gene *AOX1* is controlled at the level of transcription. In methanol-grown cells ~5% of poly(A)$^+$ RNA is from *AOX1*; however, in cells grown on most other carbon sources, the *AOX1* message is undetectable.[36] The regulation of the *AOX1* gene involves a two step mechanism: a repression/derepression mechanism plus an induction mechanism. The expression of a foreign gene in *P. pastoris* requires three basic steps: (1) the insertion of the gene into an expression vector; (2) introduction of the expression vector into *P. pastoris* genome; and (3) examination of potential expression strains for the foreign gene product. A variety of P. *pastoris* expression vectors and host strains are available. All expression vectors have been designed as *Escherichia coli/P. pastoris* shuttle vectors, containing an origin of replication for plasmid maintenance in *E. coli* and markers functional in one or both organisms. Most expression vectors have an expression cassette composed of a 0.9 kb fragment from *AOX1* composed of the 5′ promoter sequence and a second short *AOX1*-derived fragment with sequences required for transcription termination, as well as many cloning sites for gene insertion and an antibiotic resistant gene for positive selection in *E. coli* and *P. pastoris* (Figure 2-2). One set of vectors the pPICZ series are used for intracellular expression whereas pPICZα vectors designed for extracellular expression of the foreign protein. The pPICZα and the pPICZ vectors contain the *sh ble* gene from *Streptoalloteichus hindustanus* which codes for Zeocin™ resistance for selection in *E. coli* and *P. pastoris*. The vector pPICZα A has selectable markers for both *E. coli* and *P. pastoris*, and is easier to manipulate.

The pPICZα A vector

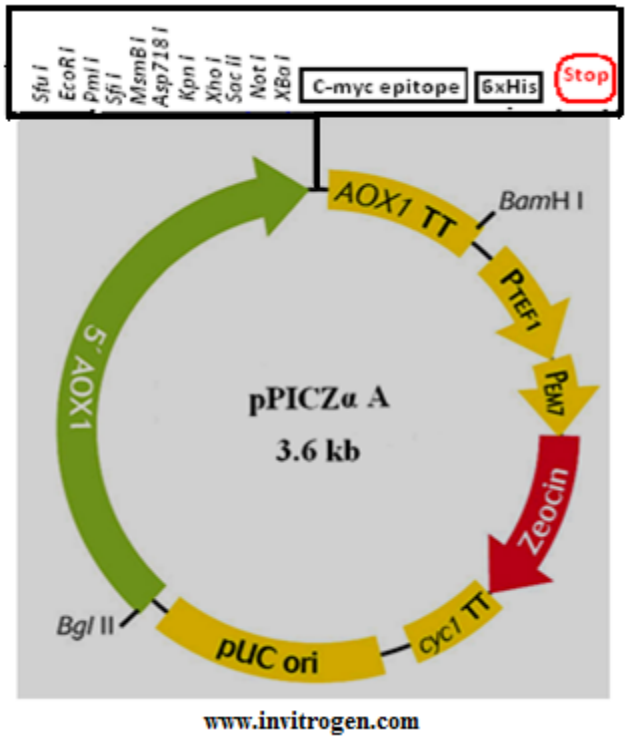

Figure 2-2: Yeast vector pPICZα A (3.6 kb) and *Xho* I and *Xba* I cloning sites.

The possible recombinant strains that can be generated are the Mut^+ (methanol utilization plus) and Mut^s (methanol utilization slow). The Mut^+ is referred to as the wild type because of its ability to grow on methanol as the only carbon source. Mut^s is due to the loss of the *AOX1* gene, which results in slow growth on methanol medium. The Mut^+ phenotype, X-33 strain of *P. pastoris*, a wild type strain and pPICZα A has been used for this research project.

Transformation of *Pichia* Strains

Restriction digest by BstX1

To linearize plasmids for transformation into *Pichia pastoris* strains, 10 µg of isolated plasmid was digested with 2 µL BstX1 buffer, 0.2 µL of 10 mg/ml BSA, 1 µL BstX1 (Promega), and sterile water to bring the total volume to 20 µL. The reaction mixture was incubated at 50 °C for 2 hours, 5 µL aliquots of which were analyzed on a 1% agarose gel to check the digest for complete linearization. The enzyme was heat inactivated at 65 °C for 10 minutes after the vector had been completely linearized.

Preparation of P. pastoris competent cells

10 mL of yeast peptone dextrose medium (YPD) containing 1% Zeocin™, was inoculated with a single colony of *Pichia* strains X-33, GS115 and KM71H. Samples were grown overnight at 28 °C in a shaking incubator. Cells were diluted from the overnight cultures to an optical density (OD_{600}) of 0.2 in a 10 mL sample of fresh YPD. Cells were then grown for 5 hours at 28 °C in a shaking incubator until the OD_{600} reached 1.0. Cells were centrifuged at 2500 rpm for 5 minutes at room temperature. The pellets were resuspended in 1 mL of solution I (1 M sorbitol, 10 mM bicine, 3% (v/v) ethylene glycol, 5% (v/v) DMSO, pH 8.0). The cells were centrifuged again, and resuspended in 1 mL of solution I as competent cells. 50 µL aliquots of cells were distributed into 1.5 mL microcentrifuge tubes then wrapped in several layers of paper towels for storage in the -80 °C freezer.

Transformation of P. pastoris

For each transformation, one tube (50 µL) of competent cells was thawed at room temperature and 5 µg of linearized plasmid and 1 mL of solution II (40% PEG 1000, 0.2 M

bicine, pH 8.0) were added to each tube. The tubes were flicked vertically several times to mix thoroughly. The transformation reactions were incubated in a water bath for 1 hour at 30 °C with mixing by flicking the tubes every 15 minutes to enhance transformation efficiency. The cells were then heat shocked at 42 °C in a heat block for 10 minutes. Each tube content was then split into two (approximately 525 µL for each tube) and 1 mL of YPD medium was added to each. The cells were incubated for 1 hour at 30 °C to allow expression of Zeocin™ resistance. Cells were then centrifuged for 5 minutes at 5000 rpm at room temperature (AccuSpin™ Micro, Fisher Scientific). Each tube of cells were resuspended in 500 µL of solution III (0.15 M NaCl, 10 mM bicine, pH 8.0) and combined in one tube. The combined cells are pelleted at 5000 rpm for 5 minutes at room temperature and resuspended in 150 µL of solution III. The entire transformation solutions were then platted on YPDS (1% yeast extract, 2% peptone, 2% dextrose, 1 M sorbitol, 2% agar) plates containing 1% Zeocin™ and grown for 3 days at 30 °C.

Analysis of P. pastoris transformants

Ten colonies of the Zeocin™ resistant *Pichia* transformants were selected on MDH (minimal dextrose histidine medium) and MMH (minimal methanol histidine medium) to confirm the Mut phenotype. Using a sterile toothpick, a single colony of one transformant was patched in a regular pattern on both the MDH and MMH plates with the MMH plates being the first to be patched. A new toothpick was used each time for all the ten colonies. Plates were incubated for two days at 30 °C. To differentiate between Mut^+ and Mut^s, two controls, GS115/Mut^s albumin and GS115/pPICZ/*lacZ* Mut^+, were also streaked as two lines on the plates.

PCR analysis of transformants

10 mL of YPD medium containing 100 µg/mL of Zeocin™ was inoculated with a single colony of the transformants from MDH/MMH plates. The cells were grown overnight in a

shaking incubator at 30 °C. 1.5 mL of the overnight yeast culture was spun at 13,000 rpm for 1 minute to pellet the cells. 300 µL of acid-washed 425-600 micron glass beads, 200 µL of lysis buffer (2% Triton X-100, 1% SDS, 2% 100mM NaCl, 1% 10 mM Tris-HCl pH 8.0, 5% 10 mM EDTA), and 200 µL of PCIA (50% phenol, 48% chloroform, 2% isoamyl alcohol) were added to the cells to resuspend the pellets. The mixture was centrifuged for 5 minutes at 13,000 rpm which produced a layer of glass beads at the bottom, an opaque PCIA layer in the middle, and a clear aqueous layer on the top. The aqueous top layer is transferred into a new 1.5 ml microcentrifuge tube. 200 µL buffer TE (100 mM Tris-HCl pH 8.0, 10 mM EDTA) was added to the original tube, and then vortexed and centrifuged for 5 minutes at 13,000 rpm. The top aqueous layer was added to the previous aqueous layer. 400 µL of PCIA was added to the combined aqueous layer, vortexed and centrifuged for 5 minutes. The top aqueous layer was transferred to another tube and 400 µL of PCIA was added, vortexed, and centrifuged. This was repeated until the opaque layer disappeared. The supernatant was transferred into another tube and 40 µL of 3 M sodium acetate (pH 5.2), plus 1 mL of 100% ethanol was added. The samples were stored at -20 °C for 30 minutes and then centrifuged at high speed for 10 minutes. The supernatant was discarded and the pellet washed with 200 mL 70% ethanol and vacuum dried. The pellets were dissolved in 20 µL 1 x TE and 1 µL RNase. 2 µL of extracted DNA was used for the PCR reactions. The PCR reaction included 10 µL Green Master Mix (Promega), 50 ng of plasmid DNA, 1 µL 10 µM 5' AOX1, 1 µL 10 µM 3' AOX1 and nuclease-free water to adjust the volume to 20 µL. The thermal cycle program consisted of 95 °C melting for 2 minutes followed by 1 minute denaturation at 95 °C, annealing at 50 °C for 30 seconds, 1 minute extension at 72 °C for 30 cycles, and 10 minutes final extension allowed at 72 °C completing transcription. The samples were analyzed on 1% agarose gel run at 85 V for 75 minutes.

Small-Scale Protein Expression

Small scale protein expression was performed in different yeast media to determine which one gave the best expression of protein.

Expression in BMGY/BMMY media

Colonies were selected from yeast strains X-33 (PeYX1, PeYX2, PeYX3, PeYX4, PeYX5), GS115 (PGs1, PGs2, PGs3, PGs4, PGs5) and KM71H (PkM1, PkM2, PkM3, PkM4, PkM5) cultured over two days on YPDS plates containing 100 mg/mL Zeocin™. The colonies were grown in 25 mL of BMGY (1% yeast extract, 2% peptone, 10% 100 mM potassium phosphate buffer pH 6.0, 1.34% YNB (yeast nitrogen base), 4 x 10^{-5} % biotin, 1% glycerol) in a 250 mL baffled flasks. The cell culture was grown overnight at 28 °C in a shaking incubator at 300 rpm until the cultures reached an OD_{600} of 2.0-6.0 at approximately 16-18 hours. The cells were harvested by centrifuging at 11,000 rpm for 5 minutes at 4 °C. The cell pellets were resuspended in 150 mL BMMY (1% yeast extract, 2% peptone, 10% 100 mM potassium phosphate buffer pH 6.0, 4 x 10^{-5} % biotin, 1.34% YNB, 1% methanol) medium to induced protein expression. 0.01% of antifoam agent (Sigma) was added to prevent frothing and to enhance the exchange of air. 100-150 mL of culture was placed in 1 L sterile baffled flasks, labeled, covered with two layers of sterile cheesecloth and grown approximately four days. 500 µL methanol was added every 24 hours to maintain induction and 1 mL of expression culture was collected into 1.5 mL microcentrifuge tubes at time points of 6, 12, 24, 48, 72, 96, and 120 hours. Samples were centrifuged at 13,000 rpm at room temperature for 1 minute. Both supernatant and pellets were immediately frozen on dry ice/ethanol and stored in the -80 °C

freezer for further analysis of secreted protein, to determine the optimum time for expression of the secreted protein.

Expression in BMGH/BMMH media

25 mL of BMGH medium (10% 100 mM potassium phosphate buffer pH 6.0, 1.34% YNB, 4 x 10^{-5} % biotin, 1% glycerol, 0.004% histidine) was inoculated with 50 µL of cells stored in 15% glycerol in a 250 mL baffled flasks. The culture was grown overnight with shaking at 250 rpm at 28 °C. The cells were harvested at 11,000 rpm for 5 minutes at 4 °C when an OD_{600} of 2.0-6.0 was reached in approximately 16 – 18 hours.

The cells were resuspended in 150 mL BMMH medium (10% 100 mM potassium phosphate, buffer pH 6.0, 1.34% YNB, 4 x 10^{-5} % biotin, and 1% methanol, 0.004% histidine) to induce expression. The sample was added to a sterile 1 L baffled flask with addition of 0.01% antifoaming agent to prevent frothing. The culture was covered with two layers of sterile cheesecloth and grown four approximately four days in a shaking incubator at 300 rpm at 28 °C. 500 µL aliquots of methanol were added after every 24 hours to maintained induction. Aliquots of 1 mL of the sample were collected at time points 6, 12, 24, 48, 72, 96, and 120 hours into a 1.5 mL microcentrifuge tube, and then centrifuged at 13,000 rpm. The supernatant was decanted into a clean microcentrifuge tube, and both supernatant and pellets were immediately frozen on dry ice/ethanol and stored at -80 °C. The supernatants were analyzed for extracellular expression of proteins and the pellets analyzed for intracellular expression, using the Bradford protein assay and SDS-PAGE.

Expression in MGYH/MMH media

To express the transformed yeast strains in a non buffered medium, 25 mL of MGYH medium (1.34 % YNB, 1 % glycerol, 4 x10^{-5} % biotin, 0.004 % histidine) was inoculated with colonies of yeast transformants in 250 mL sterile baffled flasks, grown at 28 ˚C in a shaking incubator at 300 rpm until the OD_{600} reached 2.0-6.0, after 16 hours. The cells were harvested by centrifugation at 11,000 rpm for 5 minutes at 4˚C. The cells were resuspended in 149 mL MMH (minimal methanol histidine) to obtain an OD_{600} of 1.0. The culture was then placed in a sterile 1 L baffled flask and antifoaming agent (0.01%) was added to avoid frothing. The cells were grown for four days in a shaking incubator (300 rpm). 500 µL aliquots of 100 % methanol were added every 24 hours to maintain induction. At the time points 6, 12, 24, 48, 72, 96, and 120 hours, 1 mL aliquots of culture were transferred into 1.5 mL microcentrifuge tubes, and then centrifuged for 1 minute at room temperature. Both pellets and supernatant were frozen on dry ice/ethanol and saved in the -80 °C freezer for analysis of levels of protein expression using Bradford assay and SDS-PAGE.

Analysis by Bradford assay

The Bradford dye-binding assay is a colorimetric assay used for measuring total protein concentration. It involves the binding of Coomassie Brilliant blue dye to protein in an acidic medium shifting the absorbance from 465 nm to 595 nm with a color change from brown to blue. Coomassie Bradford assay reagent (100 mg of Brilliant Blue G-250, 50 mL methanol, 100 mL of 85% w/v phosphoric acid, DI H_2O for total of 1 L) was used to determine the total protein concentration using bovine serum albumin (BSA) of a known concentration as the standard. A set of protein standards were prepared using 1 mg/mL BSA in (Table 2-1).

Table 2-1: BSA (1mg/mL) Samples for Standard Curve

Tube	Volume of BSA (µL)	Volume of DI water (µL)	Coomassie reagent (mL)
Blank	0	100	3.0
A	10	90	3.0
B	30	70	3.0
C	50	50	3.0
D	70	30	3.0
E	100	0.0	3.0

100 µL of each BSA standard was pipetted into an appropriately labeled test tube and 3.0 mL of Coomassie reagent was added to each tube, vortexed, and incubated for 10 minutes at room temperature. The spectrophotometer (HP 845 UV-Visible system) was zeroed using the blank and the measurement taken at 595 nm. Absorbances of all standards were measured at the same wavelength, and a standard curve of absorbance versus BSA concentration was prepared. The total protein concentrations of the supernatants obtained in all the expression yeast cultures were measured to quantify levels of protein expression.

Analysis by SDS-PAGE

The supernatants collected at various time points in all the media were analyzed by SDS-PAGE. The supernatants stored in the freezer were thawed to room temperature and placed on ice. The samples for SDS-PAGE were prepared by using 15% Tris-HCl gel (Bio-Rad laboratories). The gels were set in the SDS chamber and the chambers were filled with electrophoresis running buffer (0.25 M Tris, 1.92 M glycine, 1% SDS, pH 8.3). 10 µL of each sample was mixed with 10 µL of protein gel loading buffer 2x (Amresco), boiled for 4 minutes

and insoluble material was removed by centrifugation using a table-top centrifuge. 20 µL of each sample was loaded in the wells, and the gel was run at 200 V for 70 minutes. The gel was then stained in Coomassie brilliant blue R-250 for 1 hour, washed with DI water five times, destained in a destaining solution (5% methanol, 7% acetic acid, 88% DI water), and then fixed in fixing solution (50% methanol, 10% acetic acid, 40% DI water) for preservation.

Lysozyme enzyme assay

To examine whether the lysozyme mutant protein was present in an active form in the supernatant a lysozyme enzyme assay was performed using *Micrococcus lysodeikticus*. The assay relies on the rate of lysis of *M. lysodeikticus* as suggested by Shugar.[39] One unit of enzyme is equal to a decrease in turbidity of *M. lysodeikticus* suspension of 0.001 per minute at 450 nm and 25 °C. The *M. lysodeikticus* cell suspension was prepared by adding 0.3 mg/mL of cells to 0.1 M potassium phosphate buffer (pH 7.0). The suspension was allowed to incubate for 1 hour at room temperature. The assay was performed on a HP 845 UV-Visible spectrophotometer at a wavelength of 450 nm. The sample cell was held at 25 °C using a circulating water bath. 2.9 mL of suspended *M. lysodeikticus* was pipetted into a disposable cuvette and incubated for 4 minutes to equilibrate the cells. Blank readings were obtained using the equilibrated sample. 100 µL of lysozyme standard in various concentrations was added and the absorbance recorded every 10 seconds for 4 minutes. The native lysozyme enzyme starting at 10 mg/mL was diluted several times until the corrected rate of 0.02 ΔA_{450}/minute was obtained. The corrected rate was calculated using zero order kinetics from 40-240 seconds. The supernatant samples were assayed alongside the standards to avoid variation in cell substrate.

Scale-up of Expression

The scale-up expression was begun once the optimization using small-scale expression had been achieved. Colonies which did express the protein were grown in large quantities in the respective media for further studies. 25 mL of BMGY was inoculated with 50 µL of the highest expresser yeast cells (Gps1) saved in 15% glycerol in a 250 mL baffled flask. The cell culture was incubated in a shaking incubator (250 rpm) at 28 °C for 16 hours until the culture reached an of OD_{600} of 2.0-6.0. The cells were harvested with sterile centrifuge bottles at 4 °C and 11,000 rpm for 3 minutes. The supernatant was decanted and the cell pellet resuspended in BMMY to an OD_{600} of 1.0. The culture was then aliquoted into 300 mL volumes into several 2 L baffled flasks, covered with two layers of cheesecloth and returned to the incubator to continue to grow till the time of induction was reached (24 hours). The sample was centrifuged at 13,000 rpm at 4 °C for 10 minutes and the pellets were discarded. Supernatant was concentrated from 600 mL to 4 mL, for purification experiments.

Section III: Purification and Characterization of Mutant Protein

Preliminary purification with gel filtration chromatography was carried out to purify the mutant protein. 100 g of Sephacryl™ S-100 was soaked in 200 mL of water overnight to get rid of all preserving solution (20 % ethanol). The water was drained by decanting. 200 mL of buffer (20 mM potassium phosphate, 0.4 M NaCl, pH 6.0) was added to the gel beads to form a thick slurry. The gel was packed in a 90 cm x 1.5 cm column to a height of ~60 cm. Two column volumes of buffer were allowed to run through it to equilibrate the stationary phase. A 2 mL concentrated sample of the mutant lysozyme protein (0.54 mg/mL) was applied onto the column bed. The protein was allowed to elute with the same buffer of 20 mM plus 0.4 M NaCl,

pH 7.0 at 75 drops per test tube, and the absorbance of each tube was determined at 280 nm and a graph of A_{280} versus test tube number was plotted. Fractions were pooled under peaks with the highest absorption and further concentrated using Amicon concentrators (MWCO 3000 Da). The fractions are dialyzed to remove low molecular weight proteins and salts and then concentrated to a desired volume (2 mL-4 mL) using Amicon concentrators.

Separation by HPLC

HPLC samples were prepared by obtaining aliquots of protein samples dialyzed against 20 mM potassium phosphate buffer and 0.4 M NaCl, centrifuged at high speed and the supernatant decanted into a clean microcentrifuge tube. The precipitate formed at centrifugation was dissolved in HPLC buffer A (20 mM potassium phosphate, pH 6.0), centrifuged and the supernatant added to the previous one. The HPLC column was flushed with 2 column volumes of the high salt buffer, buffer B (20 mM potassium phosphate, 0.4 M sodium chloride, pH 6.0), and equilibrated for 15 minutes with the low salt buffer, buffer A in an isocratic mode. The column was then equilibrated with high salt buffer B and low salt buffer A at a gradient of 10% for 15 minutes at a flow rate of 1.00 mL/min. 500 µL of native lysozyme at 4 mg/mL was first loaded onto the cation exchange column (polyCAT A™). The protein was eluted in 40 minutes with the linear gradient to 100% B, and the data collected from 0-40 minutes. Native lysozyme samples were run before any of the mutant protein was injected. Samples were injected every 75 minutes. Various concentrations of salt in buffer B was employed to ensure complete elution of the mutant protein, since its elution time was lower than the anticipated time.

Samples obtained from the size exclusion chromatography were analyzed for protein detection, quantification, purity, and activity.

CHAPTER III: RESULTS

Section: I Generation of the Mutant Gene, Transformation of *E. coli* and *P. pastoris*

The mutant gene (H15S) was isolated from pCR®4-TOPO® and was purified and amplified and used as the lysozyme mutant gene DNA template. Figure 3-1 illustrates the digested gene on 1% agarose gel showing a band of the right size (400 bp). The gene was then sub-cloned into the *Pichia* vector pPICZα A, followed by transformation into competent One Shot® TOP10 *E. coli* cells. The plasmid was isolated and 10 µL of sample obtained from the plasmid purification was analyzed by 1% agarose gel electrophoresis in 1 X TAE buffer. The gel was run at 85 V for 75 minutes and then soaked in ethidium bromide in 1 X TAE buffer for 15 minutes and analyzed by the Stratagene imaging system EagleSight™ (Figures 3-2 and 3-3).

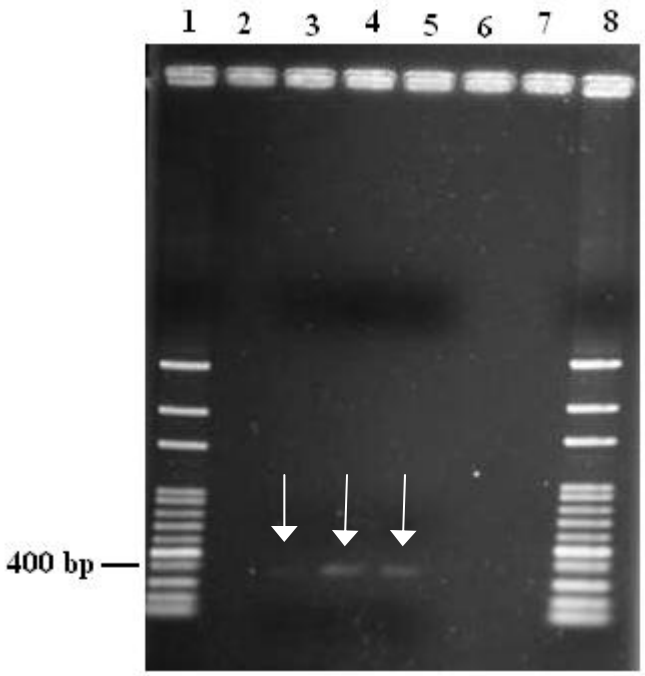

Figure 3-1: 1% agarose gel of *Xho* I digested mutant H15S cloned into pCR®4-TOPO®. Lane 1, 100 bp ladder; Lanes 3 and 4, and 5 H15S mutant gene from three different colonies.

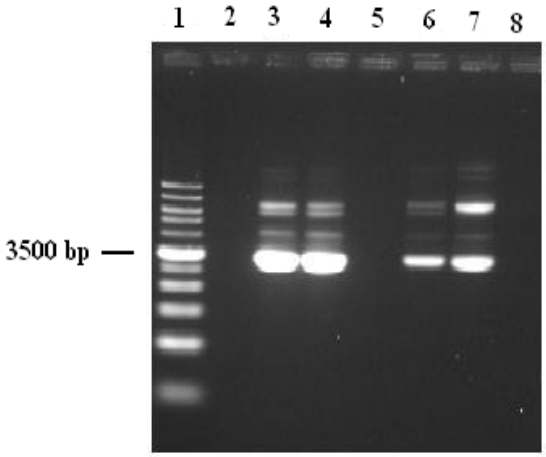

Figure 3-2: 1% agarose gel showing the isolated pPICZα A, H15S plasmid clones. Lane 1, 1 kb ladder; Lane 3, EcoxA1; Lane 4, EcoxB2; Lane 6, EcoxC3; and Lane 7, EcoxD4.

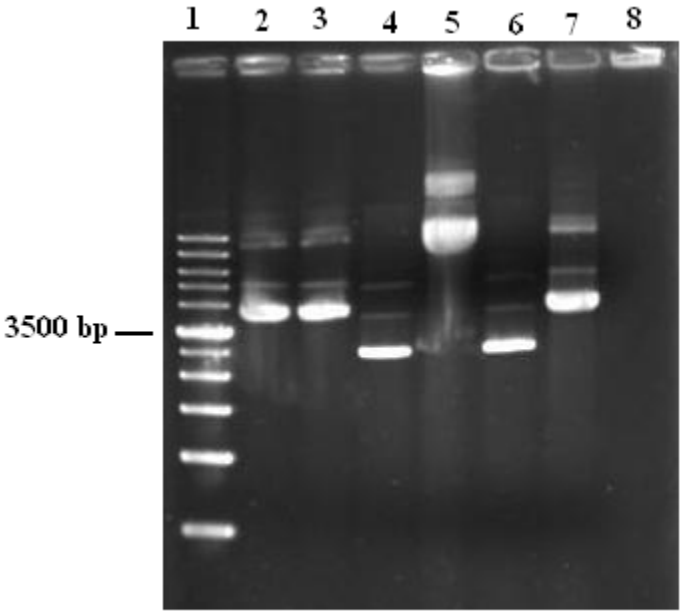

Figure 3-3: 1% agarose gel showing isolated pPICZα A, H15S plasmid clones. Lane 1, 1 kb ladder; Lane 2, EcoxE5; Lane 3, EcoxF6; Lane 4, EcoxG7, Lane 5, EcoxH8; Lane 6, EcoxI9, and Lane 7, EcoxJ10.

Plasmids isolated from colonies EcoxA1, EcoxC2, EcoxE5, EcoxF6, EcoxH8, and EcoxJ10 were analyzed for insertion of the gene using PCR. The PCR product was run on 1% agarose gel electrophoresis at 85 V for 75 minutes and stained with ethidium bromide in 1 x TAE buffer. The PCR product of the plasmid included nucleotides of the pPICZα A from the 5' *AOX1* and 3' *AOX1* primers and the inserted gene. Figures 3-4 and 3-5 illustrate PCR product run on 1% agarose gel showing the band of the right size (1000 bp).

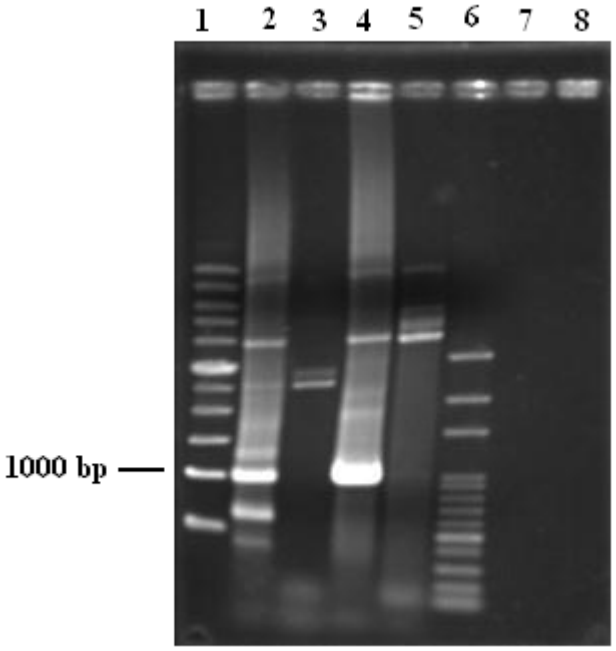

Figure 3-4: 1% agarose gel of the PCR products using pPICZα A plus the H15S gene as template. Lane 1, 1 kb ladder; Lane 2, EcoxA1; Lane 3, EcoxB2; Lane 4, EcoxC3; Lane 5, EcoxD4; and Lane 6, 100 bp ladder.

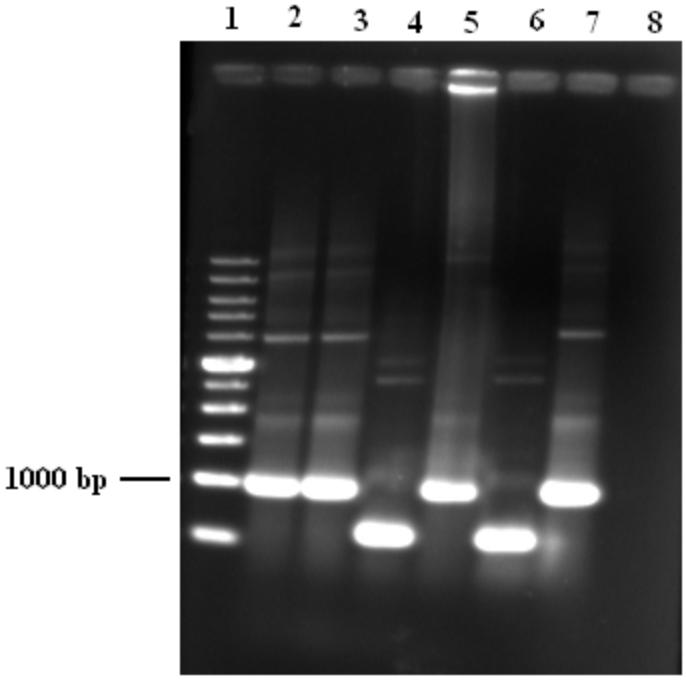

Figure 3-5: 1% agarose gel showing the PCR products of plasmids isolated from colonies 5 to 10. Lane 1, 1 kb ladder; Lane 2, EcoxE5; Lane 3, EcoxF6; Lane 4, EcoxG7; Lane 5, EcoxH8; Lane 6, EcosI9; Lane 7, EcoxJ10.

Colonies EcoxA1, EcoxC3, EcoxE5, EcoxF6, EcoxH8 and EcoxJ10 were sequenced before transforming into *Pichia* to confirm that the gene was in frame with the α-factor signal sequence, using the sequencing primers *5′ AOX1* and *3′ AOX1*. The primers are designed to amplify the gene along with the sequences coding for the gene's native sequencing signal that is the α-factor signal of the vector. The electropherogram data obtained from plasmids isolated from transformed colonies, indicated that the gene had been incorporated in frame with the α-factor signal sequence, and the mutation at position 15 points to the fact that alteration of histidine 15 (codon CAC) to serine 15 (codon AGC) had occurred (Figure 3-6).

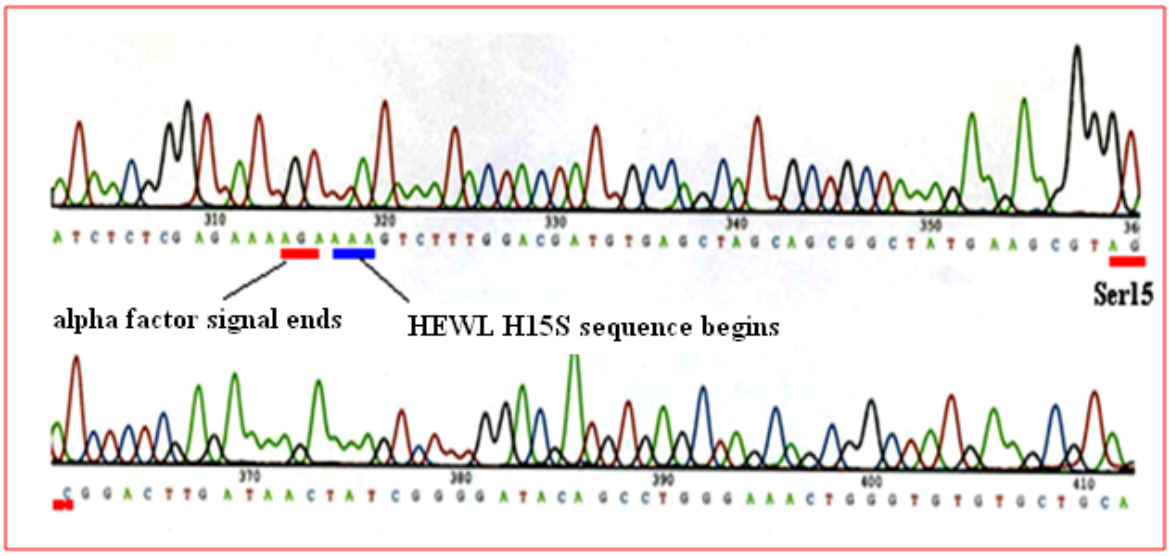

Figure 3-6: Partial electropherogram of the gene sequence with codons AGC encodes for serine.

10 µg of pPICZα A-H15S was linearized by *BstXI* (Figure 3-7) which was then integrated into the *Pichia pastoris* genome by the EasyComp™ transformation method. Ten colonies were selected after the transformation of the yeast cell. This was followed by the isolation of the genomic DNA from the cells, which was subsequently analyzed by PCR. The PCR analysis revealed a band of 1000 bp of one of the colonies (GPs1) indicating a successful integration of the cloned plasmid into the yeast DNA (Figure 3-8).

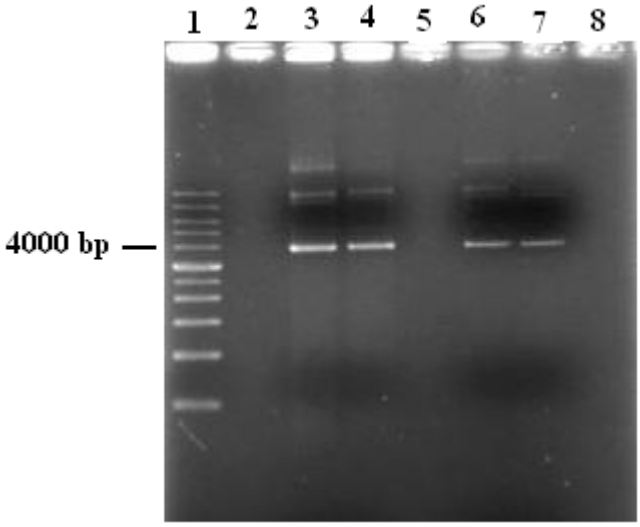

Figure 3-7: 1% agarose gel of linearized pPICZα A-H15S. Lane 1, 1 kb ladder; Lane 3, plasmid isolated from EcoxA1; Lane 4, plasmid isolated from EcoxD4, Lane 6, EcoxE5; and Lane 7 EcoxJ10.

Plasmids from colonies EcoxA1 and EcoxD4 digested with *BstX1* produced an intense band at 4000 bp. The digested DNA from these two was used to transform competent *P. pastoris* strains X-33, KM71H, and GS115. The positive integrants selected on YPDS plates were analyzed for the integrated gene and subsequent expression of the mutant protein. Figure 3-8 is a 1% agarose gel showing the PCR product of the yeast genomic DNA with a band size of ~1000 bp. Colony GPs1 of the GS115 strain was successfully transformed and that was used to begin the small-scale expression of protein.

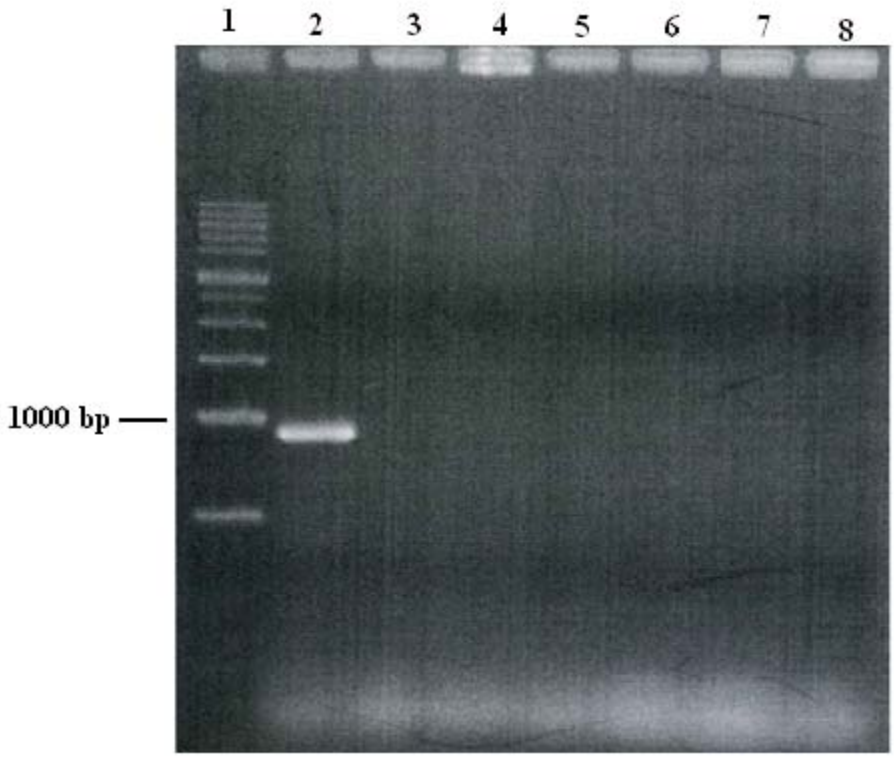

Figure 3-8: PCR product of the isolated yeast genomic DNA. Lane 1, 1 kb ladder; Lane 2, transformed GS115 strain, (GPs1).

Section II: Expression of Protein in *P. pastoris*

Small-scale expression

GPs1 was grown in three different media to determine the optimal conditions to express the mutant protein. The secretion of the mutant protein in shake-flask cultures of the media was investigated by the Bradford protein assay and SDS-PAGE. The secreted protein concentrations (mg/mL) in the various media were estimated from the standard curve of absorbance versus concentration of BSA in µg (Figure 3-9).

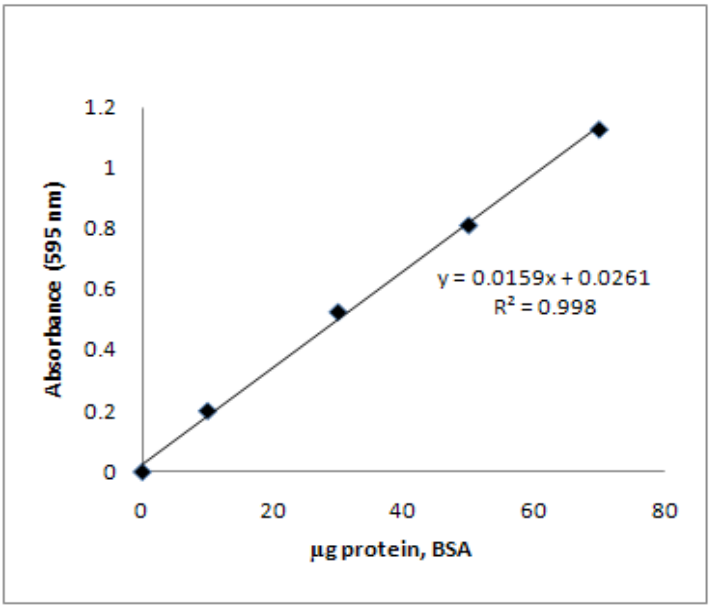

Figure 3-9: Standard curve of absorbance at 595 nm versus concentration in µg of BSA.

The concentration of the supernatant fractions collected every 24 hours was estimated (Table 3-1) to determine the amount of secreted protein at the various time points. This was necessary to optimize the expression of the mutant protein in large shake-flask cultures.

Table 3-1: Measurements of concentrations in the various media at different time points

BMGY/BMMY					
Time (hours)	24	48	72	96	120
Abs at 595 nm	0.3573	0.3375	0.3866	0.3986	0.3709
Protein conc.(mg/mL)	0.199	0.1856	0.2177	0.2255	0.2074
BMGH/BMMH					
Time/hours	24	48	72	96	120
Abs at 595 nm	0.0141	0.0052	0.0827	0.0691	0.0571
Protein conc.(mg/mL)	0.0000	0.0000	0.0191	0.010	0.002
MGYH/MMH					
Time/hours	24	48	72	95	120
Abs at 595 nm	0.1014	0.1227	0.1105	0.1103	0.1100
Protein conc.(mg/mL)	0.0313	0.0452	0.0374	0.0371	0.0369

As shown in Table 3-1 the amount of mutant protein secreted in the media BMMY and MMH increased steadily with induction time, but shows higher concentrations at each time point for BMMY (Figure 3-10). Secretion levels were at maximum at 72 hours when BMMH was used as the growth media and then decreased. BMMY was selected as the medium for protein expression, and the induction time was pegged between 24 hours to 72 hours.

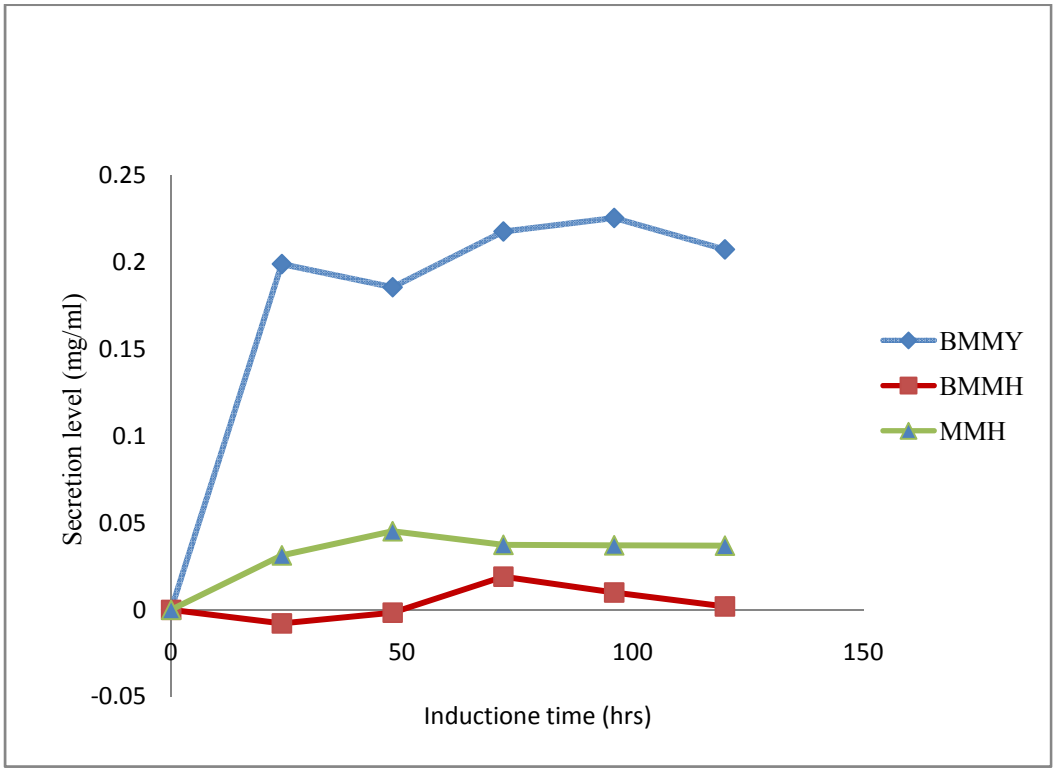

Figure 3-10: Change in concentration of secreted protein with induction time.

The variations of the protein band of the mutated lysozyme of samples collected at various time points in BMMY are shown Figure 3-11. The band density represents secretion level. The result indicated a protein band that co-migrated with the native lysozyme (14.4 kD) for the 24 hour and 72 hour cultures. Based on the results obtained from SDS-PAGE analysis,

methanol induction time for shake-flask cultures of the mutant lysozyme was set at 24 hours and 72 hours in BMMY.

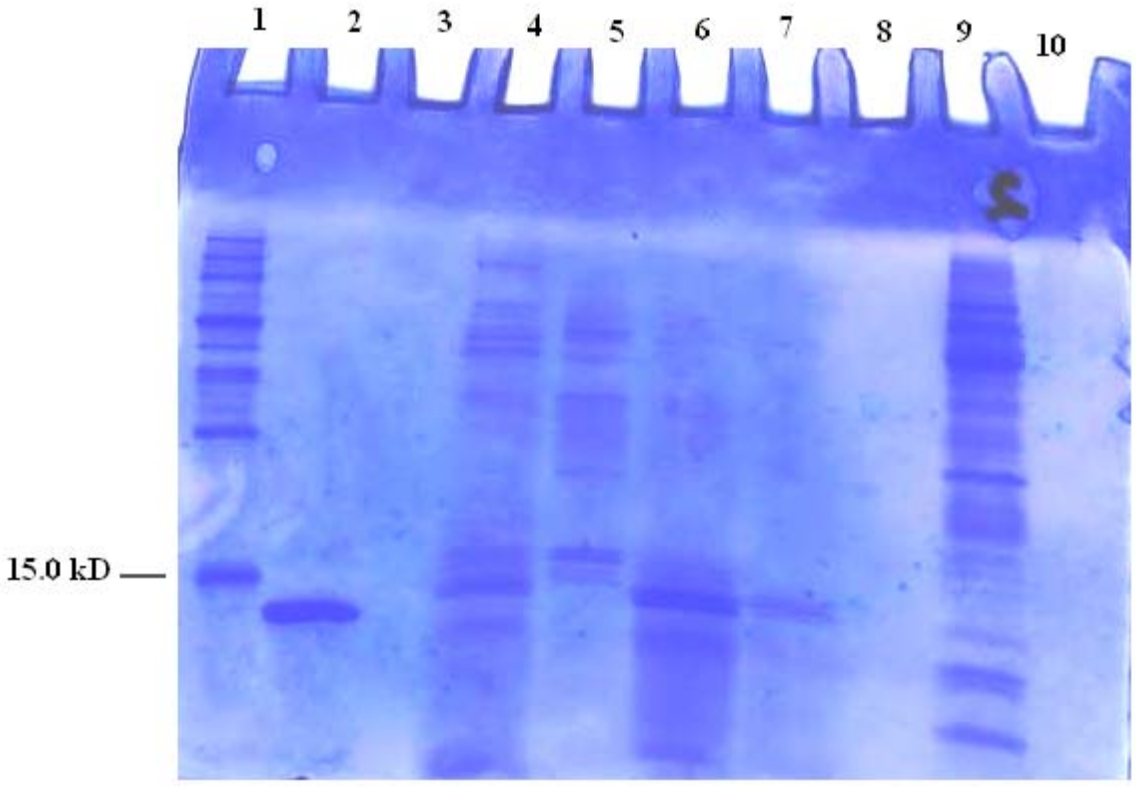

Figure 3-11: SDS-PAGE of fractions collected from BMMY over time: Lane 1, Precise™ Protein Molecular Weight; Lane 2, Lysozyme Standard; Lane 4, 24 hr; Lane 5, 48 hr; Lane 6, 72 hr; Lane 7, 96 hr; and Lane 9 120 hr.

Partially concentrated and partially purified supernatant obtained from time points 24 hours and 72 hours with 1% methanol induction was analyzed by SDS-PAGE (Figure 3-12). The results obtained in the SDS-PAGE gel indicated a strong and intense band close to the 14.4 kD band of native lysozyme was for the sample taken from the 24 hour culture as compared to 72

hour culture. As a result of this, the methanol incubation time was set at 24 hours for scale-up expression of protein.

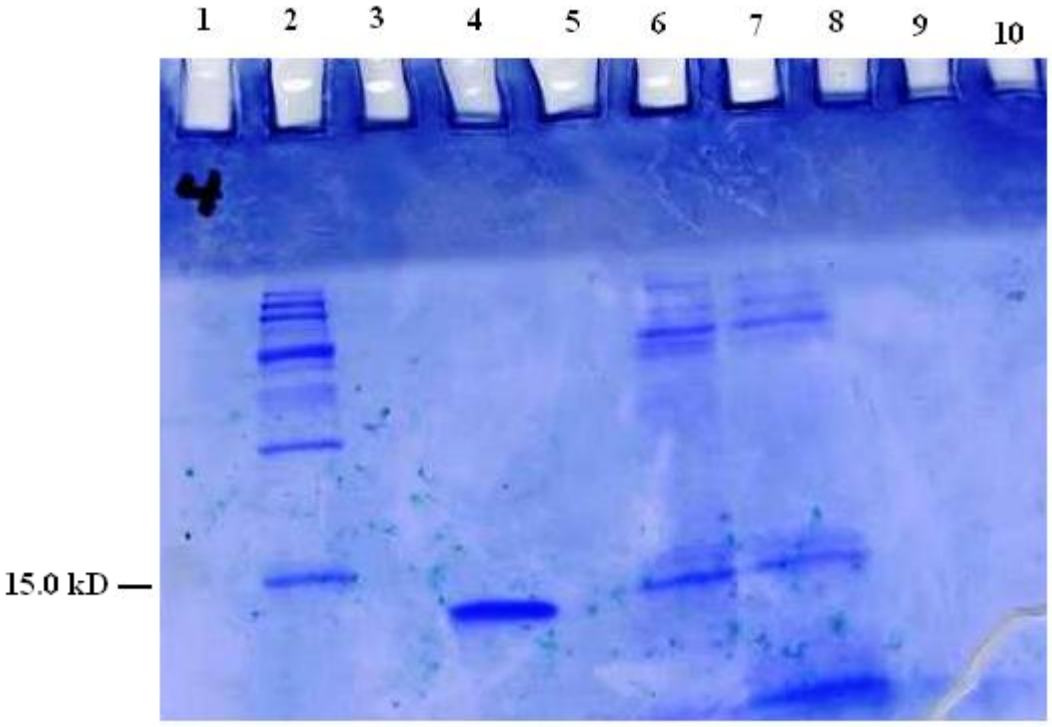

Figure 3-12: SDS-PAGE analysis of 24 and 72 hour cultures. Lane 2, molecular weight marker; Lane 4, hen egg white lysozyme; Lane 6, 24 hour supernatant; and Lane 7, 72 hour supernatant.

Scale-up expression and purification

The BMGY/BMMY growth culture gave the most promising results in small-scale expression experiments. The amount of protein secreted after 24 hours was about 0.24 mg/mL with 1% methanol induction. One liter batch cultures were grown. The supernatant collected was concentrated using the Easy Load Master Flex® equipped with Minimate™ TFF Capsule down to about 30 mL. This volume was further concentrated to between 2-4 mL using Amicon Ultra-4 (Ultracel-3k) concentrators. A Bradford assay of the concentrated sample gave a concentration of

0.43 mg/mL protein. Two milliliters of the concentrated protein was loaded onto the size exclusion column and eluted with a low salt phosphate buffer.

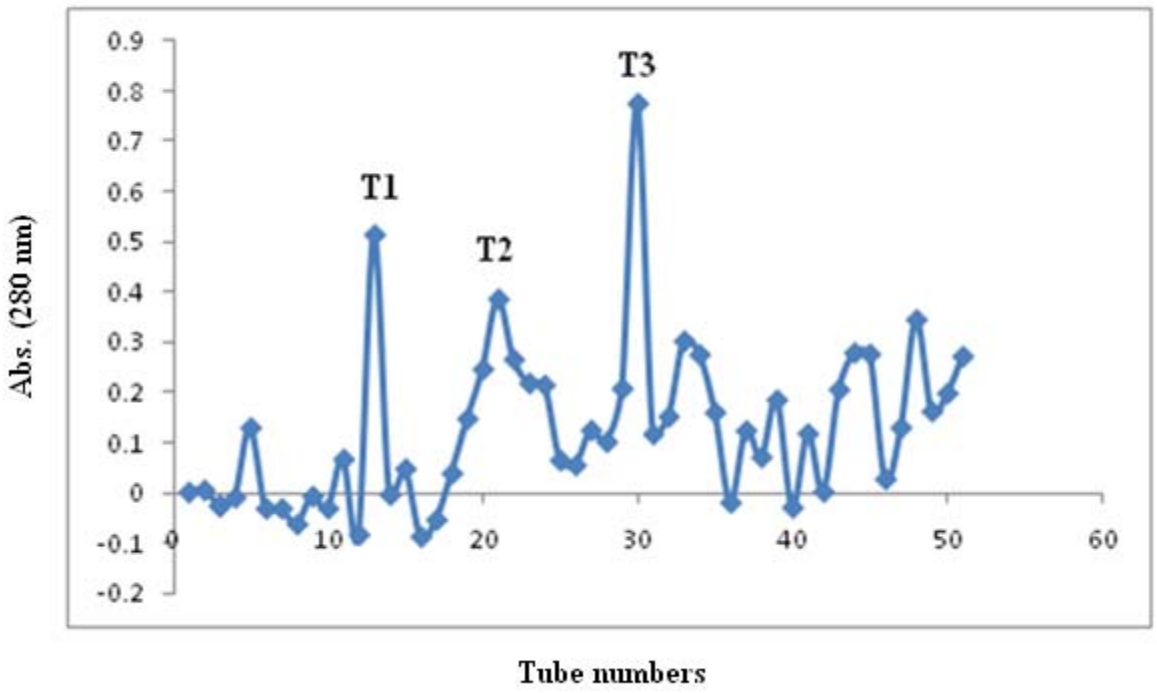

Figure 3-13: Graph of absorbance versus tube number for eluted fractions separated by; using Sephacryl™ S-100.

The adsorbed proteins were eluted with the starting buffer containing 0.17 M NaCl. 2 mL fractions were collected in each test tube. Figure 3-13 shows a plot of the absorbance at 280 nm versus tube numbers for fractions eluted from the column. Fractions in the peaks were pooled, concentrated and analyzed by SDS-PAGE (Figure 3-14).

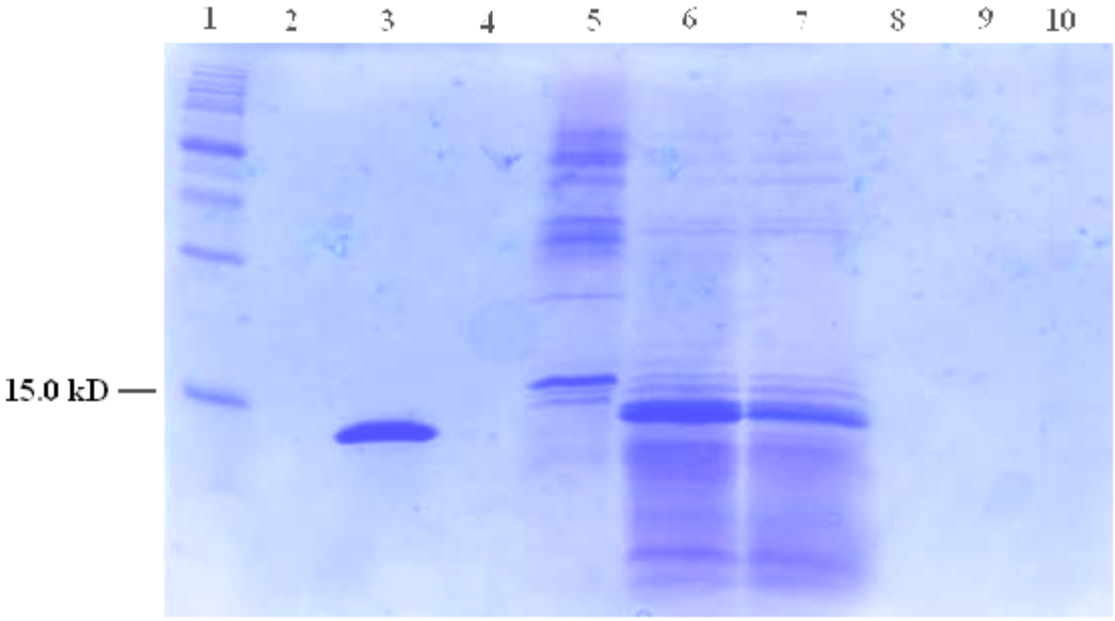

Figure 3-14: SDS-PAGE analysis of gel filtration fractions: Lane 1; protein molecular weight marker, Lane 3; hen egg white lysozyme standard, Lane 5, fractions in peak 1, Lane 6; fractions in peak 2; and Lane 7, fractions in peak 3.

As shown in lane 5 (Figure 3-14), larger molecules were observed in fractions collected under peak 1 while smaller molecules are found for fractions collected under peaks 2 and 3. To further purify the samples for HPLC analysis, fractions collected under peaks 2 and 3 were dialyzed against 20 mM potassium phosphate buffer. Precipitate formed during dialysis but was dissolved in a low salt buffer and preserved for further analysis. The supernatant and the dissolved precipitate were concentrated further down using Amicon Ultra-4 concentrators. The resultant concentrated protein solutions were washed with water to remove salts. The SDS-PAGE indicated that the precipitate that formed upon dialysis did not contain a protein with a molecule near that of lysozyme (Figure 3-15).

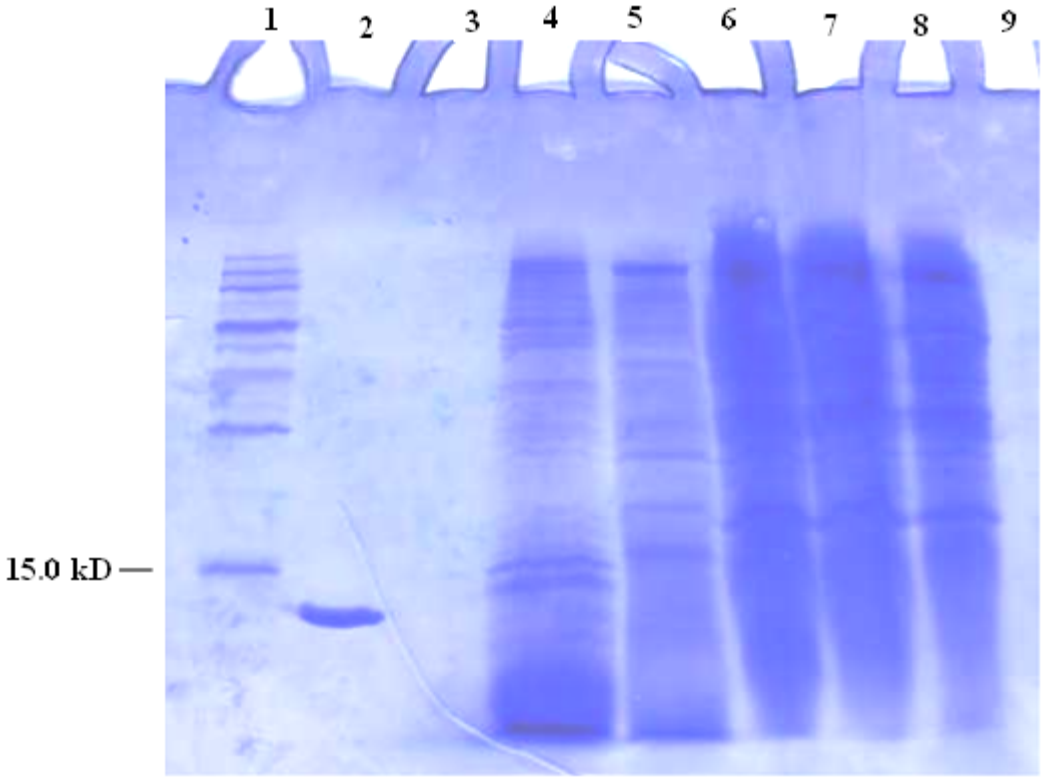

Figure 3-15: SDS-PAGE of dialyzed sample from 24 hr culture in BMMY. Lane 1, molecular weight marker; Lane 2, hen egg white lysozyme; Lane 4, crude sample; Lane 5 supernatant from dialysis; Lanes, 6, 7 and 8 precipitated molecular species dissolved in 20 mM potassium phosphate buffer

In attempts to separate the mutant protein from other molecular species, 500 µL aliquots of the crude sample, the concentrated samples from dialysis, and samples from the eluent of size exclusion chromatography were loaded onto a PolyCAT A™ column. The proteins were eluted as described in Materials and Methods. Unlike the native hen egg lysozyme, the proteins from cultured samples eluted from the column within 2 to 10 minutes and there were no representation peaks near the one for native lysozyme which eluted between 34-36 minutes (Figure 3-16)

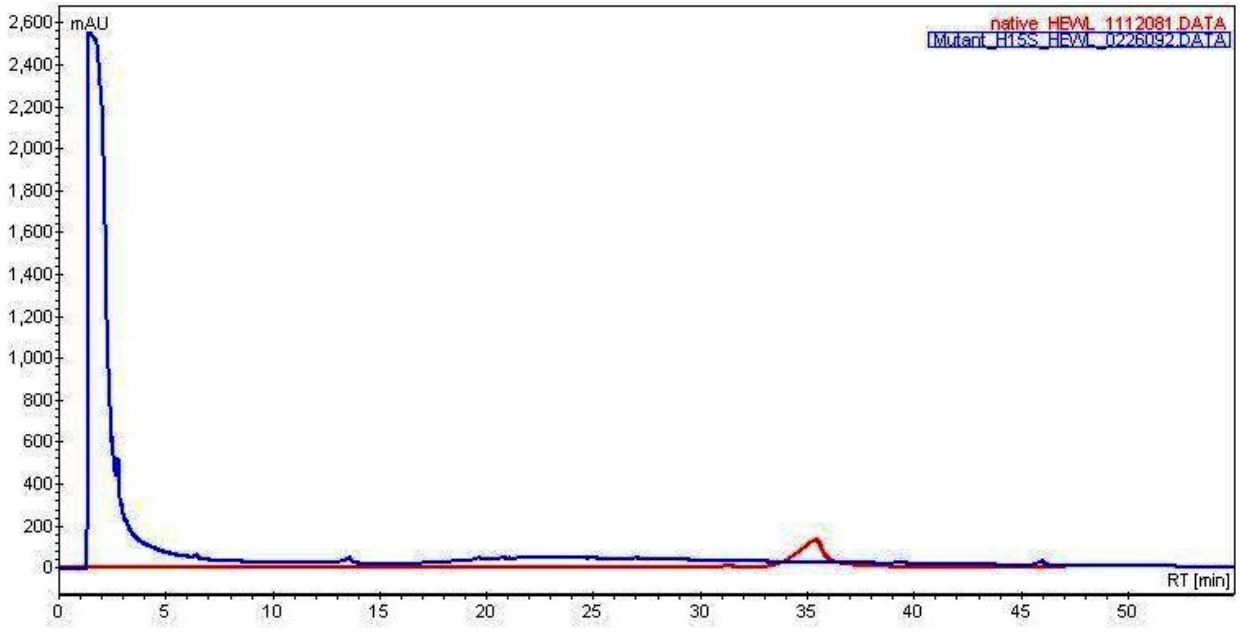

Figure 3-16: Chromatograms of native lysozyme (red line) and mutant protein (blue line) eluted with high salt phosphate buffer pH 6.0 at a flow rate of 1.00 mL/min.

Enzyme Assay

Enzyme assays were performed to determine the lytic activity of crude extracts, concentrated samples, dialyzed and partially purified samples of the mutant protein. The absorbance at 450 nm was measured every 10 seconds for a total of 4 minutes. The ΔA_{450}/minute was obtained using zero order kinetics fitting data from 40-240 seconds. The lytic activity obtained from a 100 µL aliquot of 10 µg/mL of hen egg white lysozyme was used as a control (Figure 3-17).

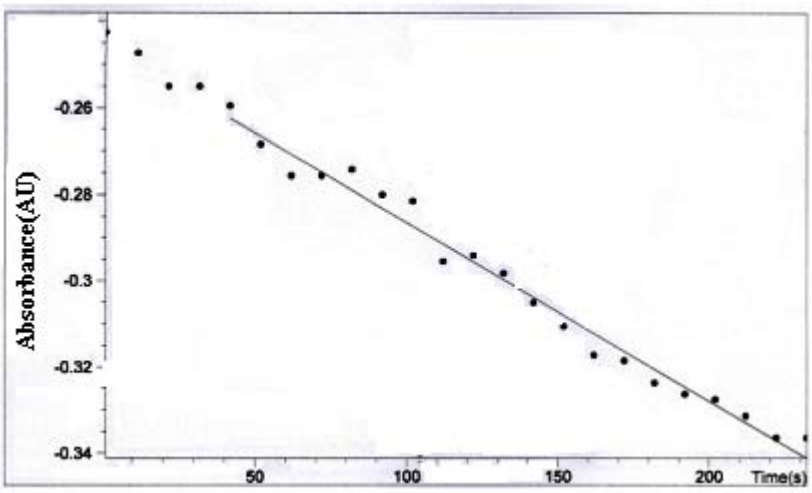

Figure 3-17: Graph of lytic activity of native hen egg white lysozyme.

Lytic activity could not be detected with 100 µL aliquots of samples collected at 48 hours, 72 hours, 96 hours and 120 hours. The 24 hour culture showed weak lytic activity when supernatant obtained from BMMY cultures were applied to *M. lysodeikticus* (Figure 3-18).

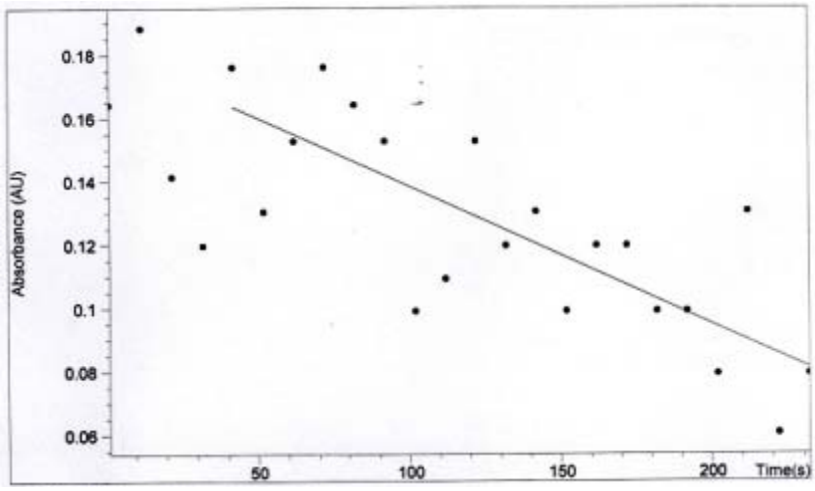

Figure 3-18: Graph of lytic activity of the crude sample from collected 24 hour culture in BMMY.

The fractions obtained from gel filtration chromatography were analyzed for enzyme activity and most failed to exhibit any lytic activity, but the concentrated fraction of peak 2, did show detectable lytic activity (Figure 3-19).

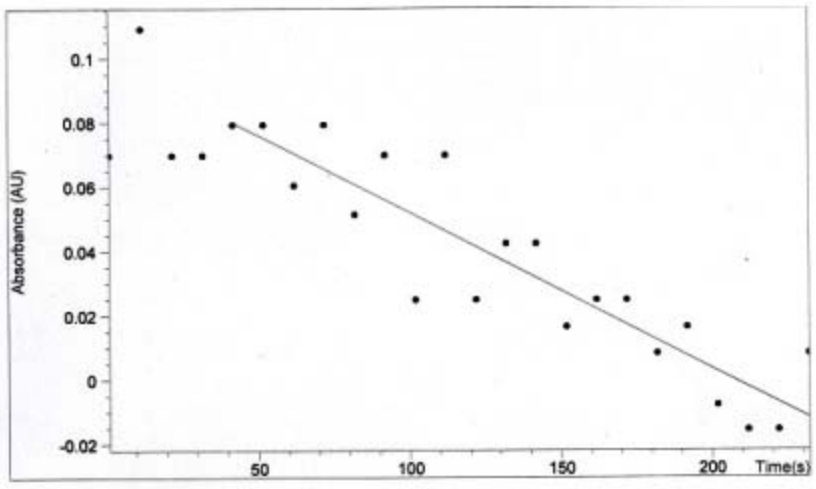

Figure 3-19: Graph of lytic activity of fractions collected in peak 2 from gel filtration chromatography.

CHAPTER IV: DISCUSSION

The perception that metal-catalyzed oxidation is a "caged" reaction has been discussed by many researchers.[46] The "caged" system of the reaction occurs when metal ions bind in a protective pocket on the protein's surface providing protection from anti-oxidants for the production of ROS. Other lines of evidence also suggest the availability of a metal-binding residue alone is sufficient to initiate metal catalyzed oxidation. To examine the importance of primary as opposed to the tertiary structure in site-specific oxidation, a single mutant of hen egg white lysozyme (HEWL)was generated. In the amino acid sequence of native HEWL (appendix A) His15 is found in a protective pocket (Figure 1-6), which provides protection for the production of ROS, and it becomes difficult for the antioxidant defense systems to scavenge.

HEWL was chosen as the model protein for several reasons. The enzyme is relatively small consisting of only 129 amino acid residues. It is a well characterized structure and is one of the most extensively studied proteins having been used as a model protein in various fields of protein research.[40] Several successful attempts have been made to express other forms of lysozyme in *E. coli* and *P. pastoris.* The unstable H5-lysozyme mutant protein with its hydrophobic pentapeptide (Phe-Phe-Val-Ala-Pro) at C or N-terminus has been expressed in *P. pastoris* with methanol induction. The amount of the protein secreted was 422-fold greater than that observed in *Saccharomyces cerevisiae*.[41] Mutant N^{15} enriched HEWL has also been expressed in the *P. pastoris* system.[42, 43] HEWL has been expressed in *E. coli*, however, the expression of active enzyme in *E. coli* consequently led to bacterial cell lysis due to hydrolysis of the peptidoglycan.[41, 44]

In this research study, a single site mutant of HEWL has been generated. Serine was deemed a safe substitution for histidine based on an algorithm developed by Bordo and Argos.[40]

The initial steps of the experiment involved generating the single mutant H15S gene and cloning the gene into the yeast vector pPICZα A. The *Pichia* vector cloned with the H15S was used to transform the TOP10 strain of *E. coli* for maintenance of the plasmid. The insertion of the gene into the *E. coli* cells was verified by isolating the plasmid from 1.5 mL of an overnight culture of the cells as described in Materials and Methods. The plasmid DNA was analyzed by agarose gel electrophoresis and DNA sequencing. The cloned vector was linearized and used to transform the *Pichia* strains X-33, GS115 and KM71H for the expression of the gene.

HEWL has a molecular weight of 14.4 kD; therefore, a protein band of ~14 kD was expected in the SDS-PAGE gels run with samples obtained from the various time points of 0, 24, 48, 72, 96, and 120 hours in the different media used in the expressing the mutant protein. A band of the correct size was observed when the complex buffered medium BMMY was used in the small-scale expression with culture volume of 100-150 mL. There was no visible band near 14.4 kD in the SDS-PAGE gels when samples collected from media BMMH and MMH were analyzed. The amount of protein secreted into the medium increased from zero hours and then decreased substantially after 24 hours. Lytic activity was not detected in samples collected from time points 48, 72, 96, and 120 hours. There was slight detection of lytic activity with the crude and the purified sample of the 24 hour time point (Figures 3-18 and 3-19). The lytic activity obtained for the 24 hour culture supernatant (Figure 3-18) showed greater variability as compared to the purified concentrated sample from gel filtration chromatography obtained for the same 24 hour period.

Large scale expression in BMMY medium did not produce as much protein as expected in the 24 hour culture, however, an increase of about 7.5% in terms of milligram protein was observed compared to the amount of protein obtained in the small scale expression. Samples

obtained from gel filtration were analyzed by cation exchange chromatography in an effort to separate the secreted protein from other molecular species however, there were no visible peaks that eluted close to the elution range of the native lysozyme.

Due to low levels of protein expression some parameters such as methanol concentration and incubator shaking speed were subjected to changes. The amount of methanol was increased from 1% to 2% and the rotor speed was adjusted to 350 rpm. Nevertheless, these changes did not improve the yields in protein expression. By comparison, it has been reported in the literature that ^{15}N-labeled lysozyme expression in *P. pastoris* reached 20 mg/mL in five days with 0.5% methanol induction.[42] It has also been reported that expression of H5-lysozyme in *P. pastoris* was 2.1 mg/mL after four days in BMMY medium.

In order to ensure that lower levels of secretion of the mutant protein were not due to intracellular protein accumulation, SDS-PAGE analysis was performed on cell lysates after various times of induction. In all the instances no visible band of ~14.4 kD was observed. Based on the low level of expression the vector cloned into the bacteria cell was cross checked by performing a *Xho* I digest (Figure 4-1).

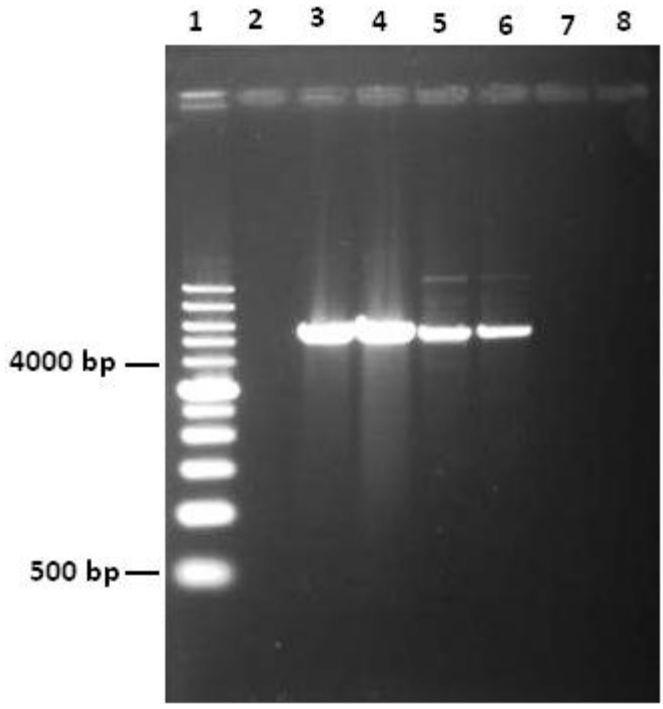

Figure 4-1: 1% agarose gel of *Xho* I digest of H15S, pPICZα A plasmid. Lane 1, 1 kb ladder; Lane 3 to Lane 6, plasmids isolated from JM110 *E. coli* strain.

The cloned plasmid used in our expression of the H15S HEWL evidently underwent a recombination event in the JM110 *E. coli* strain. This was evidenced by the size of the digested band at approximately 5500 bp. The correct band size is 4000 bp. This is a likely possibility for the low level of protein expression that has been experienced even in large cultures. Based on these results, fresh gene was acquired, re-cloned into fresh pPICZα A and the plasmid DNA used to transform fresh competent TOP10 *E. coli* to continue with the expression as discussed in chapter III.

Different ways of increasing high yield secretion of the mutant protein

The chromatographic and electrophoretic data clearly indicated that the mutant protein was secreted extracellularly, but expression levels were relatively low therefore, better expression conditions are necessary to express the mutant protein in high yields. There are several options that exist to improve expression levels such as generating strains containing multiple integrants of the vector or creating multiple copies of the recombinant gene integrated into the yeast genome.[31] Another alternative is to introduce the *P. pastoris* glyceradehyde-3-phosphate (GAP) promoter into the expression vector instead of the *AOX1* promoter. The GAP promoter has been reported to secrete the recombinant esterase into the external medium to a concentration of 7 mg/mL.[45] The advantage of using *GAP* is that methanol is not required for induction, nor is it necessary to shift cultures from one carbon source to another, making strain growth more straightforward.

One of the reasons for the low level of protein expression in large scale cultures can be attributed to relatively low bio-mass accumulation in shake-flask cultures (OD_{600} 2.5-3.0). *P. pastoris* yeast thrives well in fermenter cultures with good bio-mass accumulation; therefore, using fermentors may also increase protein expression.

Conclusions:

In this study the mutant lysozyme (H15S) was expressed using the *P. pastoris* expression system. The PCR and sequence analysis results indicated that the H15S mutant gene was successfully cloned into the *P. pastoris* genome. The analysis of supernatant from shake-flask cultures on SDS-PAGE revealed a band that migrated

with the native lysozyme (control), and was assumed to be the mutant lysozyme. Fractions obtained in the elution peak T2 from gel filtration were prepared and applied to SDS-PAGE. The SDS-PAGE investigation also revealed two protein bands near the migration position of the native lysozyme. Expression of the H15S gene in various media was carried out according to standard protocols. Buffered complex media with methanol was found to be suitable for the expression of the protein. Expression appeared to be maximal with 1% methanol induction at 24 hour time point and a shaker speed of 300 rpm. However, since the secretion level of the mutant protein was too low (< 1mg/mL) to carry out metal-catalyzed oxidation studies, it would be prudent to find alternative purification techniques or different routes to enhance expression using *P. pastoris.* For example (a) additional studies aimed at optimizing culture conditions for the GS115 strain which has a mutation in the histidinol dehydrogenase gene (*His4*) and the X-33 strain which is the wild-type with Mut^+ phenotype in which the integrated gene will be found upstream of the 5' *AOX1* region. (b) generating a strain with multiple integrated copies of the expression cassette. A strain that contains multiple integrated copies of the expression cassette can sometimes yield more heterologous protein than single-copy strains.[31]

References

1. Lushchak, V. I. (2007) *Biochemistry (Moscow)*, **72**, 809-827.

2. Reddy, P. H. (2008) *Neuromolecular Medicine* **10**, 291-315.

3. Muller, F. L., Florian, L., Lustgarten, Michael, S., Jang, Youngmok, Richardson, A., Arlan, Van, R. H., Holly (2007) *Free Radical Biology & Medicine*. **43**, 477-503.

4. Halliwell, B., Gutteridge, J. M. C. (1985) *Molecular Aspects Medicine*, **8**, 89-193.

5. Li, S., Shöneich, C., Borchardt, R. T. (2004) *Biotechnology & Bioengineering*, **48**, 5, 490-500.

6. Cheeseman, K. H., Slater, T. F. (1993) *British Medical Bulletin*, **49**, 481-493.

7. Halliwell, B. (1993) *Toxicology & Industrial Health*, **9**, 1-21.

8. Stohs, J. S. (1995) *Basic Clinical Physiology Pharmacology*, **6**, 205-228.

9. Farber, J. L. (1995) *Environmental Health Perspective*, **103** (Supply 1), 17-19.

10. Kamkofer, M. (2000) *Reproduction in Domestic Animals*, **35**, 229-233.

11. Halliwell, B. (1987) *FASEB* **1**, 358-364.

12. Davies, J. M. (2005) *Biochemical Biophysical Acta*, **1703**, 93-109.

13. Yi, Sun, (1990) *Free Radical Biological Medical Science*, **8**, 583-599.

14. Halliwell, B. (1992) *Journal of Neurochemistry*, **59**, 1609-1623.

15. Sies, H. (1997) *Experimental Physiology*, **82**, 291-295.

16. De Silva, D. M., Aust, S. D. (1992) *Journal of Physiology Pharmacology*, **71**, 715-720.

17. Halliwell, B., Cross, E. C. (1994) *Environmental Health Perspective (Supplement 10)*, **102**, 5-10.

18. Stadtman, E. R., Levine, R. L. (2003) *Amino Acids*, **25**, 207-218.

19. Stadtman, E. R, Oliver, C. N. (1991) *Biological Chemistry*, **266**, 2005-2008.

20. Oliver, C. N., Levine, R. L., Stadtman, E. R. (1981) *Metabolic Interconversion of Enzymes* (Holzer, H., ed.), 259-268.

21. Schöneich, C. (2001) *Journal of Pharmacology and Biomedical Analogy*, **21**, 1093-1097.

22. Pérez, L. M., Milkiewicz, P., Ahmed-Choudhumy, J., Roma, G. M. (2006) *Free Radical Biology & Medicine*, **40**, 2005-2017.

23. Di Monte, D., Ross, D., Bellomo, G., Eklow, L., Orrenius, S., Arch. (1984) *Biochemical Biophysics*, **235**, 334-342.

24. Agil, A., Fuller, J. C., Jialal, I. (1995) *Clinical Chemistry* **41**, 220-225.

25. Oliver, G. N., Ahn, B. W., Moerman, E. J., Golstein, S., and Stadtman, E. R. (1987) *Journal of Biological Chemistry*, **262**, 5488-5491.

26. Miyata, T., Inagi, R., Aslahi, K., Yamada, Y., Horie, K., Sakai, H., Uchida, K., and Kurokawa, K. (1998) *FEBS Letters*, **437**, 24-28.

27. Chandhuri, R. A., Dewaal, E. M., Pierce, A., Van Remmen, H., Ward, W. F., and Richardson, A. (2006) *Mechanism of Aging and Development*, **127**, 869-861.

28. Giulivi, C., Traaseth, N. J., and Davies, J. A. (2003) *Amino Acids*, **25**, 227-232.

29. Giulivi, C., and Davies, K. J. A. (1994) *Methods in Enzymology*, **233**, 363-371.

30. Giulivi, C., and Cadenas, E. (1998) *Free Radical Biology and Medicine*, **24**, 269-279.

31. Heinecke, J. W. (2002) *Free Radical Biology and Medicine*, **32**, 1090-1101.

32. Garrison, W. M. (1987) *Chemical Reviews*, **87**, 381-398.

33. Schuessler, H., and Schilling, K. (1984) *International Journal of Radical Biology*, **45**, 267-281.

34. Uchida, K., Kato, Y., and Kawakishi, S. (1990) *Biochemical and Biophysical Research Communications*, **169**, 265-271.

35. Hovorka, S.W., Williams, T. D., and Schöneich, C. (2002) *Analytical Biochemistry*, **300**, 206-211.

36. Cereghino, J. L., and Cregg, J. M. (2000) *FEMS Microbiology Reviews*, **24**, 45-66.

37. Couderc, R., and Baratti (1980) *Agricultural and Biological Chemistry*, **44**, 10, 2279-2289.

38. Woo, A. H., Jeong, W., Chang, T. S., Park J. K., Park, J. S., Yang, S. J., and Rhee S. G. (2005) *Journal of Biological Chemistry*, **280**, 3125-3128.

39. Shugar, D. (1952) *Biochemical Biopsychology Acta*, **8**, 302-309.

40. Bordo, D., Argos, P. (1991) *Journal of Molecular Biology* **217**, 721-729.

41. Liu, T. S., Saito, A., Azakami, H., and Kato, A. (2003) *Protein Expression and Purification,* **27**, 304-312.

42. Mine, S., Ueda, T., Hashimoto, Y., Tanaka, T., Imoto, T. (1999) *FEBS Letters*, **448**, 33-37.

43. Spencer, J. A., Jeenes, J. D., Mackenzie, A. D., Haynie, T. D., Archer, B. D. (1998) *European Journal of Biochemistry* **258**, 107-112.

44. Fischer, B., Perry, B., Philips, G., Summer, I., Goodenough, P. (1993) *Applied Microbiology and Biotechnology* **39**, 537-540

45. Delroisse, M. J., Dannau, M., Gilsoul, J. J., Mejdoub, T. E., Destain, J., Portelle, D., Thonart, P., Haubruge, E., Vandenbol, M. (2005) *Protein Expression and Purification,* **42**, 286-294.

46. Bridgewater, J., Lim, J., Vachet, W. R. (2006) *Journal of American Society for Mass Spectrometry*, **17**, 1552-1559.

47. Uchida, K. (2003) *Amino Acids*, **25**, 249-257.

Appendix A

Hen Egg White Lysozyme Gene and Amino Acid Sequence

1-10	AAA	GTC	TTT	GGA	CGA	TGT	GAG	CTA	GCA	GCG
	Lys	Val	Phe	Gly	Arg	Cys	Glu	Leu	Ala	Ala
11-20	GCT	ATG	AAG	CGT	CAC	GGA	CTT	GAT	AAC	TAT
	Ala	Met	Lys	Arg	His	Gly	Leu	Asp	Asn	Tyr
21-30	CGG	GGA	TAC	AGC	CTG	GGA	AAC	TGG	GTG	TGT
	Arg	Gly	Tyr	Ser	Leu	Gly	Asn	Trp	Val	Cys
31-40	GCT	GCA	AAA	TTC	GAG	AGT	AAC	TTC	AAC	ACC
	Ala	Ala	Lys	Phe	Glu	Ser	Asn	Phe	Asn	Thr
41-50	CAG	GCT	ACA	AAC	CGT	AAC	ACC	GAT	GGG	AGT
	Gln	Ala	Thr	Asn	Arg	Asn	Thr	Asp	Gly	Ser
51-60	ACC	GAC	TAC	GGA	ATC	CTA	CAG	ATC	AAC	AGC
	Thr	Asp	Tyr	Gly	Ile	Leu	Gln	Ile	Asn	Ser
61-70	CGC	TGG	TGG	TGC	AAC	GAT	GGC	AGG	ACT	CCA
	Arg	Trp	Trp	Cys	Asn	Asp	Gly	Arg	Thr	Pro
71-80	GGC	TCC	AGG	AAC	CTG	TGC	AAC	ATC	CCG	TGC
	Gly	Ser	Arg	Asn	Leu	Cys	Asn	Ile	Pro	Cys
81-90	TCA	GCC	CTG	CTG	AGC	TCA	GAC	ATA	ACA	GCG
	Ser	Ala	Leu	Leu	Ser	Ser	Asp	Ile	Thr	Ala
91-100	AGC	GTG	AAC	TGT	GCG	AAG	AAG	ATC	GTC	AGC
	Ser	Val	Asn	Cys	Ala	Lys	Lys	Ile	Val	Ser
101-110	GAT	GGA	AAC	GGC	ATG	AAC	GCG	TGG	GTC	GCC
	Asp	Gly	Asn	Gly	Met	Asn	Ala	Trp	Val	Ala
111-120	TGG	CGC	AAC	CGC	TGC	AAG	GGT	ACC	GAC	GTC
	Trp	Arg	Asn	Arg	Cys	Lys	Gly	Thr	Asp	Val
121-129	CAG	GCG	TGG	ATC	AGA	GGC	TGC	CGG	CTC	TAG
	Gln	Ala	Trp	Ile	Arg	Gly	Cys	Arg	Leu	Stop

Note:	CTG	TAA	GTC	to	CT***C***	TA***G***	***AG***C	
	Leu	Stop	Val		Leu	Stop	Ser	